

LOAN DOCUMENT

PHOTOGRAPH THIS SHEET

DTIC ACCESSION NUMBER

LEVEL

INVENTORY

WL-TR-96-2091

DOCUMENT IDENTIFICATION

DISTRIBUTION STATEMENT A
Approved for public release
Distribution Unlimited

DISTRIBUTION STATEMENT

ACCESSION DATA	
NTIS	GRASS
DTIC	TRAC
UNANNOUNCED	
JUSTIFICATION	
BY	
DISTRIBUTION/	
AVAILABILITY CODES	
DISTRIBUTION	AVAILABILITY AND/OR SPECIAL
A-1	
DISTRIBUTION STAMP	

H
A
N
D
L
E

W
I
T
H

C
A
R
E

DATE ACCESSED

DATE RETURNED

DTIC QUALITY INSPECTED 1

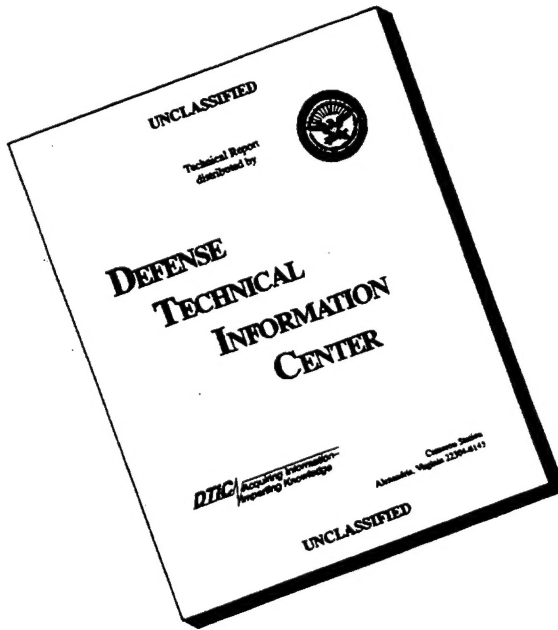
A-1
19960812 168

DATE RECEIVED IN DTIC

REGISTERED OR CERTIFIED NUMBER

PHOTOGRAPH THIS SHEET AND RETURN TO DTIC-FDAC

DISCLAIMER NOTICE



**THIS DOCUMENT IS BEST
QUALITY AVAILABLE. THE
COPY FURNISHED TO DTIC
CONTAINED A SIGNIFICANT
NUMBER OF PAGES WHICH DO
NOT REPRODUCE LEGIBLY.**

WL-TR-96-2091



**TURBULENT HEAT TRANSFER
INVESTIGATION: TURBULENCE LENGTH
SCALES AND TURBINE HEAT TRANSFER**

**Jason Sharp
Pete Harris**

3 MAY 1996

FINAL REPORT 1 NOVEMBER 1995--9 JULY 1996

Approved for public release; distribution unlimited

**AERO PROPULSION & POWER DIRECTORATE
WRIGHT LABORATORY
AIR FORCE MATERIEL COMMAND
WRIGHT-PATTERSON AIR FORCE BASE, OH 45433-7650**

This paper is declared a work of the U.S. Government and as such is not subject to copyright protection in the United States

NOTICE

WHEN GOVERNMENT DRAWINGS, SPECIFICATIONS, OR OTHER DATA ARE USED FOR ANY PURPOSE OTHER THAN IN CONNECTION WITH A DEFINITELY GOVERNMENT-RELATED PROCUREMENT, THE UNITED STATES GOVERNMENT INCURS NO RESPONSIBILITY OR ANY OBLIGATION WHATSOEVER. THE FACT THAT THE GOVERNMENT MAY HAVE FORMULATED OR IN ANY WAY SUPPLIED THE SAID DRAWINGS, SPECIFICATIONS, OR OTHER DATA, IS NOT TO BE REGARDED BY IMPLICATION, OR OTHERWISE IN ANY MANNER CONSTRUED, AS LICENSING THE HOLDER, OR ANY OTHER PERSON OR CORPORATION; OR AS CONVEYING ANY RIGHTS OR PERMISSION TO MANUFACTURE, USE, OR SELL ANY PATENTED INVENTION THAT MAY IN ANY WAY BE RELATED THERETO.

THIS REPORT IS RELEASABLE TO THE NATIONAL TECHNICAL INFORMATION SERVICE (NTIS). AT NTIS, IT WILL BE AVAILABLE TO THE GENERAL PUBLIC, INCLUDING FOREIGN NATIONS.

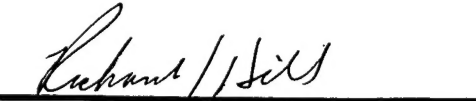
THE TECHNICAL REPORT HAS BEEN REVIEWED AND IS APPROVED FOR PUBLICATION.



RICHARD B. RIVIR
Manager, Aerothermal Research
Turbine Branch
Turbine Engine Division
Aero Propulsion & Power Directorate



CHARLES D. MACARTHUR
Chief
Turbine Branch
Turbine Engine Division
Aero Propulsion & Power Directorate



RICHARD J. HILL
Chief of Technology
Turbine Engine Division
Aero Propulsion & Power Directorate

IF YOUR ADDRESS HAS CHANGED, IF YOU WISH TO BE REMOVED FROM OUR MAILING LIST, OR IF THE ADDRESSEE IS NO LONGER EMPLOYED BY YOUR ORGANIZATION PLEASE NOTIFY WL/POTT, WPAFB OH 45433-7650 TO HELP MAINTAIN A CURRENT MAILING LIST.

REPORT DOCUMENTATION PAGE

*Form Approved
OMB No. 0704-0188*

Public reporting burden for this collection of information is estimated to average 1 hour per response, including the time for reviewing instructions, searching existing data sources, gathering and maintaining the data needed, and completing and reviewing the collection of information. Send comments regarding this burden estimate or any other aspect of this collection of information, including suggestions for reducing this burden, to Washington Headquarters Services, Directorate for Information Operations and Reports, 1215 Jefferson Davis Highway, Suite 1204, Arlington, VA 22202-4302, and to the Office of Management and Budget, Paperwork Reduction Project (0704-0188), Washington, DC 20503.

1. AGENCY USE ONLY (Leave blank)			2. REPORT DATE 3 May 1996		3. REPORT TYPE AND DATES COVERED Final 1 Nov 95 - 9 Jul 96	
4. TITLE AND SUBTITLE Turbulent Heat Transfer Investigation: Turbulence Length Scales and Turbine Heat Transfer			5. FUNDING NUMBERS PE 61102F JON 2307S315			
6. AUTHOR(S) Jason Sharp, Pete Harris						
7. PERFORMING ORGANIZATION NAME(S) AND ADDRESS(ES) Aero Propulsion & Power Directorate Wright Laboratory Air Force Materiel Command Wright-Patterson Air Force Base, OH 45433-7650			8. PERFORMING ORGANIZATION REPORT NUMBER			
9. SPONSORING / MONITORING AGENCY NAME(S) AND ADDRESS(ES) Aero Propulsion & Power Directorate Wright Laboratory Air Force Materiel Command Wright-Patterson Air Force Base, OH 45433-7650 POC: Richard B Rivir, WL/POTT, 513-255-5132			10. SPONSORING / MONITORING AGENCY REPORT NUMBER WL-TR-96-2091			
11. SUPPLEMENTARY NOTES						
12a. DISTRIBUTION / AVAILABILITY STATEMENT APPROVED FOR PUBLIC RELEASE; DISTRIBUTION IS UNLIMITED				12b. DISTRIBUTION CODE		
13. ABSTRACT (Maximum 200 words) This experiment was designed to study the effects of turbulent length scales on turbine blade heat transfer in a steady state cascade wind tunnel. Turbine blade heat transfer is of interest due to the beneficial effects engine performance that can arise from improvements in turbine blade cooling and design. Turbulence in this experiment was generated by means of passive grids in the upstream flow. This experiment uses a steady state liquid crystal in combination with resistance heating to measure heat transfer. The liquid crystals provide surface temperature data and the resistance heating in the blade can be computed from measured currents to determine heat transfer. When combined with flow data taken with a hot film this allows for conclusions on the effects of length scales on heat transfer to be made. This experiment showed that the turbine blade heat transfer exhibited the trends already investigated for turbulence intensity, namely an increase in heat transfer with increased turbulence, the forward movement of boundary layer transition and the elimination of pressure side spanwise variations. Comparison of the two different length scales at the same turbulence intensity showed that the length scale evidenced no affect on transition location or post-transition heat transfer. However, pre-transition heat transfer was significantly increased as the integral length scale decreased from 2.78 to 0.51. This demonstrates that smaller more compact eddies in the turbulent flow have a more significant impact on increasing heat transfer than do larger eddies of the same intensity.						
14. SUBJECT TERMS					15. NUMBER OF PAGES 53	
					16. PRICE CODE	
17. SECURITY CLASSIFICATION OF REPORT UNCLASSIFIED		18. SECURITY CLASSIFICATION OF THIS PAGE UNCLASSIFIED		19. SECURITY CLASSIFICATION OF ABSTRACT UNCLASSIFIED		20. LIMITATION OF ABSTRACT SAR

GENERAL INSTRUCTIONS FOR COMPLETING SF 298

The Report Documentation Page (RDP) is used in announcing and cataloging reports. It is important that this information be consistent with the rest of the report, particularly the cover and title page. Instructions for filling in each block of the form follow. It is important to stay **within the lines** to meet **optical scanning requirements**.

Block 1. Agency Use Only (Leave blank).

Block 2. Report Date. Full publication date including day, month, and year, if available (e.g. 1 Jan 88). Must cite at least the year.

Block 3. Type of Report and Dates Covered.

State whether report is interim, final, etc. If applicable, enter inclusive report dates (e.g. 10 Jun 87 - 30 Jun 88).

Block 4. Title and Subtitle. A title is taken from the part of the report that provides the most meaningful and complete information. When a report is prepared in more than one volume, repeat the primary title, add volume number, and include subtitle for the specific volume. On classified documents enter the title classification in parentheses.

Block 5. Funding Numbers. To include contract and grant numbers; may include program element number(s), project number(s), task number(s), and work unit number(s). Use the following labels:

C - Contract	PR - Project
G - Grant	TA - Task
PE - Program Element	WU - Work Unit Accession No.

Block 6. Author(s). Name(s) of person(s) responsible for writing the report, performing the research, or credited with the content of the report. If editor or compiler, this should follow the name(s).

Block 7. Performing Organization Name(s) and Address(es). Self-explanatory.

Block 8. Performing Organization Report Number. Enter the unique alphanumeric report number(s) assigned by the organization performing the report.

Block 9. Sponsoring/Monitoring Agency Name(s) and Address(es). Self-explanatory.

Block 10. Sponsoring/Monitoring Agency Report Number. (If known)

Block 11. Supplementary Notes. Enter information not included elsewhere such as: Prepared in cooperation with....; Trans. of...; To be published in.... When a report is revised, include a statement whether the new report supersedes or supplements the older report.

Block 12a. Distribution/Availability Statement.

Denotes public availability or limitations. Cite any availability to the public. Enter additional limitations or special markings in all capitals (e.g. NOFORN, REL, ITAR).

DOD - See DoDD 5230.24, "Distribution Statements on Technical Documents."

DOE - See authorities.

NASA - See Handbook NHB 2200.2.

NTIS - Leave blank.

Block 12b. Distribution Code.

DOD - Leave blank.

DOE - Enter DOE distribution categories from the Standard Distribution for Unclassified Scientific and Technical Reports.

NASA - Leave blank.

NTIS - Leave blank.

Block 13. Abstract. Include a brief (*Maximum 200 words*) factual summary of the most significant information contained in the report.

Block 14. Subject Terms. Keywords or phrases identifying major subjects in the report.

Block 15. Number of Pages. Enter the total number of pages.

Block 16. Price Code. Enter appropriate price code (*NTIS only*).

Blocks 17. - 19. Security Classifications. Self-explanatory. Enter U.S. Security Classification in accordance with U.S. Security Regulations (i.e., UNCLASSIFIED). If form contains classified information, stamp classification on the top and bottom of the page.

Block 20. Limitation of Abstract. This block must be completed to assign a limitation to the abstract. Enter either UL (unlimited) or SAR (same as report). An entry in this block is necessary if the abstract is to be limited. If blank, the abstract is assumed to be unlimited.

Table of Contents

Abstract.....	i
Table of Contents	iii
List of Tables and Figures	iv
Nomenclature List.....	v
Introduction.....	1
Theoretical Background	1
Experimental Background	1
Experimental Methods	5
Experiment Setup	5
Experiment Procedure.....	11
Uncertainty Analysis.....	12
Results and Discussion.....	13
“Clean” Tunnel Configuration (No Turbulence Grid)	14
2 3/8 in Grid Configuration.....	16
1/2 in Grid Configuration.....	18
Overall Discussion.....	19
Conclusions	20
Recommendations.....	20
Acknowledgments	21
References	22
Appendix A: Heat Transfer Graphs	23
Appendix B: Heat Transfer Data Sheets	32
Appendix C: Length Scale Data Sheets.....	34
Appendix D: Uncertainty Analysis	43

List of Tables and Figures

Figure 1: Taylor-Gortler Vortices.....	2
Figure 2: Cascade Wind Tunnel Schematic	7
Figure 3: Test Section Diagram.....	7
Figure 4: Traversable Test Probe	8
Figure 5: Test Blade Setup.....	8
Figure 6: Grid of 2 3/8 in Diameter Bars	9
Figure 7: Gird of 1/2 in Diameter Bars	10
Figure 8: Uncertainty Analysis	13
Figure 9: Stagnation Point comparison.....	15
Figure 10:Clean Tunnel Comparison	16
Figure 11:Heat Transfer Comparison.....	17
Figure 12:Grid Comparison	19
Table 1: List of Equipment	10
Table 2: Clean Tunnel Flow Comparison.....	14
Table 3: 2 3/8 in Grid Comparison.....	16
Table 4: 1/2 in Grid Comparison.....	18

Nomenclature List

B ₁	- air inlet angle, degrees
B ₂	- air exit angle, degrees
B _x	- axial chord length, in
C	- degrees Celsius
e	- voltage
e ₀	- zero velocity voltage
h	- heat transfer coefficient, W/m ² K
Hz	- Hertz
I	- electric current, amps
in	- inches
K	- degrees Kelvin
k _{air}	- thermal coefficient for air, W/mK
kg	- kilogram
l	- length of gold sheet, in
m	- meters
N	- Newton, kg m/s ²
Nu	- Nusselt number
Ohm	- measure of resistance
Ohm/SQ	- resistance per square
p	- pitch distance between turbine blades, in
P _∞	- atmospheric pressure, psi
psi	- pounds per square inch
q"	- heat transfer flux, W/m ²
q _c "	- convective heat transfer flux, W/m ²
q _L "	- conductive heat transfer flux, W/m ₂
R(T)	- autocorrelation function
R _{35.7} "	- resistance per square of gold at 35.7° C, Ohm/SQ
Re	- Reynolds number
s	- seconds
S	- surface arc length, in
St	- Stanton number
T _∞	- free-stream air temperature
T _{LC}	- surface temperature of yellow liquid crystal band, C
torr	- pressure measurement also mm Hg
T _u	- longitudinal turbulence intensity (See Equation ?)
u	- local velocity fluctuation
U	- local velocity, m/s
W	- Watts
w	- width of gold film, in
x, y, z	- longitudinal, lateral, vertical axis/distances, in
ρ	- density, kg/m ³
ε	- emissivity
σ	- Stefan-Boltzman constant, W/m ² K ⁴
μ	- viscosity of air, Ns/m ²

ΔP	- dynamic pressure, torr
Λ_u	- macro or integral turbulent length scale, m
λ_u	- microscale turbulent length scale, m
δ_x	- experimental uncertainty in parameter x

Introduction

Theoretical Background

The heat transfer on turbine blades directly affects the way engine designers can develop new turbines to allow for higher turbine inlet temperatures in engines. A better understanding of turbine blade heat transfer allows for better and more efficient cooling techniques to be developed. With more efficient cooling, increases in the turbine inlet temperature can be made without advances in materials technology. Since this has a direct and beneficial effect on the engine cycle design, reflected in greater specific thrust and lower thrust specific fuel consumption, this area is of great interest to the gas turbine engine industry. If a greater understanding of the heat transfer on such blades can be reached, new and better designs can be made.

The effect of turbulence on heat transfer has been known for some time but has yet to be physically modeled with great success. There are several parameters to describe the turbulent flow that are used in this study. The first of which is turbulence intensity. Turbulence intensity in the axial direction, noted as T_u , is one of the parameters of interest in this investigation. Turbulence intensity is a method of measuring non-dimensional turbulence in a single direction. It is the fluctuating velocity expressed as a percentage of the non-fluctuating velocity. This is expressed as:

$$T_u = \frac{\sqrt{u^2}}{U} \quad [1]$$

Roach developed correlations for predicting turbulence intensity generated by passive grids (Roach 82-92). For a square mesh of square grids this correlation is Reynolds number independent. This correlation is given as:

$$T_u = C \left(\frac{x}{d} \right)^{-5/7} \quad [2]$$

[5]

is a correlation constant which for square mesh of square bars is 1.13, d is the distance or bar diameter, and x is the distance downstream of the grid (Roach 84). This equation allows for the prediction of turbulence intensity or for this study the distance downstream to achieve a desired turbulence intensity.

Parameters of interest are the micro and macro or integral length scales. The dissipation scale is the micro length scale. It may be considered a measure of the average length scale over which energy is dissipated. The integral length scale is the macro length scale. These are primarily the method in which turbulence energy is dissipated (Roach 85). They are described by the equation:

$$\frac{1}{\lambda_u} = \frac{-1}{2U} \left\{ \frac{\partial^2 R(T)}{\partial T^2} \right\}_{T=0} \quad (\text{Roach, 85}) [3]$$

$R(T)$ represents the autocorrelation function, a correlation of each point to all other points in time. The second derivative of this correlation is used to determine the slope of this function.

The integral length or macro scale may be considered to be a measure of the largest eddy length in the flow field (Roach, 85). This is found by determining the area under the autocorrelation curve as it goes from 1 to 0. This area is determined by integrating this curve as shown below. The macro length scale is defined as:

$$\Lambda_u = U \int_0^\infty R(T) dT \quad [4]$$

Determination of the free stream velocity by the pitot probe is done via the Bernoulli equation.

use heat

These may be

ignition point

inter-rotating

impinging

vortices bring

riders of

such vortices

ur at low

from forming.

transfer



The heat transfer coefficients are of direct interest to this investigation. For this study the blade will be heated by resistance heating to provide a surface temperature higher than the surrounding air temperature. This temperature difference will in turn drive convective heat transfer to occur. The amount of resistance heating can be calculated as follows:

$$\dot{q} = \frac{I^2 R_{35.7}}{w^2} \quad [6]$$

In this equation \dot{q} is the heat transfer from the blade, I is the current applied to the blade, $R_{35.7}$ is the resistance per square of the gold, and w is the width of the gold layer. This represents the total heat transfer from the blade. In order to determine the convective heat transfer which is the target of this investigation the conductive and radiative modes of heat transfer must be accounted for. Since, the construction of the turbine blade is designed to minimize conduction by using a highly insulative closed-cell foam core, that mode is assumed to be negligible. The radiative mode is calculated by the following equation:

$$\dot{q}_R = \epsilon \sigma (T_{LC}^4 - T_\infty^4) \quad [7]$$

where T is the absolute temperature in Kelvin for both cases. By subtracting these modes from the total heat transfer the conductive heat transfer can be determined.

$$\dot{q}_c = \dot{q} - \epsilon \sigma (T_{LC}^4 - T_\infty^4) - \dot{q}_R \quad [8]$$

Once the conductive heat flux is determined the conductive heat transfer coefficient can be determined as follows.

$$h = \frac{\dot{q}_c}{(T_{LC} - T_\infty)} \quad [9]$$

The next step in the process is to non-dimensionalize this coefficient. This can be reduced to either the Stanton number or Nusselt number for reporting. These two are determined as follows:

$$St = \frac{h}{\rho V_\infty c_p} \quad [10]$$

$$Nu = \frac{hB_x}{k_{air}} \quad [11]$$

The Nusselt number can be divided further by the square root of Reynolds number to remove any Reynolds number dependency in laminar flow regions.

Experimental Background

This investigation builds on work previously performed at both the United States Air Force Academy and the University of California at Davis. This work includes investigating the effects of turbulence intensity on heat transfer as well as mapping the turbulence generated by grids. Baughn et al investigated the effect of turbulence intensity in a simultaneous study at UCDavis and USAFA. Their results can be summarized as the turbulence intensity is increased from 1% to 10% the heat transfer level increases, the suction side boundary layer transition moves upstream and the spanwise variation on the pressure side disappears (Baughn, et al 12). Baughn et al also note that these results compare favorably to rotating tests performed. This helps address the concern that cascade tunnels do not address rotational effects (Baughn, et al 12).

The study of turbulent flow quality produced by grids conducted last semester by Duncan and Peterson confirmed that the work done by Roach held true for the Cascade Wind Tunnel. The results of that investigation concluded that the correlation given by Roach worked well for passive generation such as will be used in this investigation. It also noted that the use of a grid

passive generation such as will be used in this investigation. It also noted that the use of a grid perpendicular to the flow instead of parallel to the cascade had negligible effects on the turbulence generated (Duncan and Peterson 18-19). That research used a round bar generation grid and thus the correlation coefficient is Reynolds number dependent as shown in Roach (Roach 86). This research tests a square mesh of square bars which Roach found to be Reynolds number independent in the range of interest (Roach 87).

With the effect of turbulence intensity investigated by Baughn et al and the effectiveness of generating turbulence by grids established by Roach and confirmed for the USAFA tunnel by Duncan and Peterson, this investigation establishes a relationship between length scales and heat transfer. By using a turbulence intensity level of 10%, the results of this investigation can be compared to Baughn et al, to analyze the effects of length scales. The objective of this project is to determine if a relationship exists between turbulent heat transfer and micro and macro length scales. Heat transfer is tested at 10% turbulence intensity. Additionally, a clean tunnel test is performed for comparison. Length scale comparisons will allow for a better understanding of turbulent heat transfer. Length scale investigations will provide data for updating turbulent CFD codes to include length scale effects. The investigation also looks at passive turbulence generation, comparing the results to the correlations reported by Roach (Roach 82-92).

Experimental Methods

Experiment Setup

The experiment takes place in the USAF Academy Aeronautics Lab Cascade Wind Tunnel. The Cascade Wind Tunnel is designed to place a linear cascade of turbine blades in a flow which will simulate the flow over the normally rotating turbine blades. The turbines in the

turbine around the 3rd or 4th stage with Reynolds numbers around 80,000. The tunnel is a closed loop system with a heat exchanger to provide for temperature control. In the test section are seven test blades with the end walls simulating two more blade surfaces. This setup is shown in Figure 1. The blades in the test section very closely match the Langston geometry. This geometry can be seen in Langston et al, 1977 (Langston 23).

The test section has a test probe which traverses parallel to the blade plane. This probe contains a hot film sensor, pitot-static probe and a wedge probe, which is not used in this study. The pitot-static probe is connected to a pressure transducer which outputs to a torr meter as well as the IFA 100. The hot film anemometer outputs to the IFA 100 and HP 3852A. Additionally a K type thermocouple outputs to the IFA 100 allowing for temperature measurements. Data from the IFA 100 and HP 3852A are input to the P90 computer which is controlled by TV3 software, which was written in the Aero Department. This setup is designed to collect the flow data. This can be seen in Figure 2 and Figure 3.

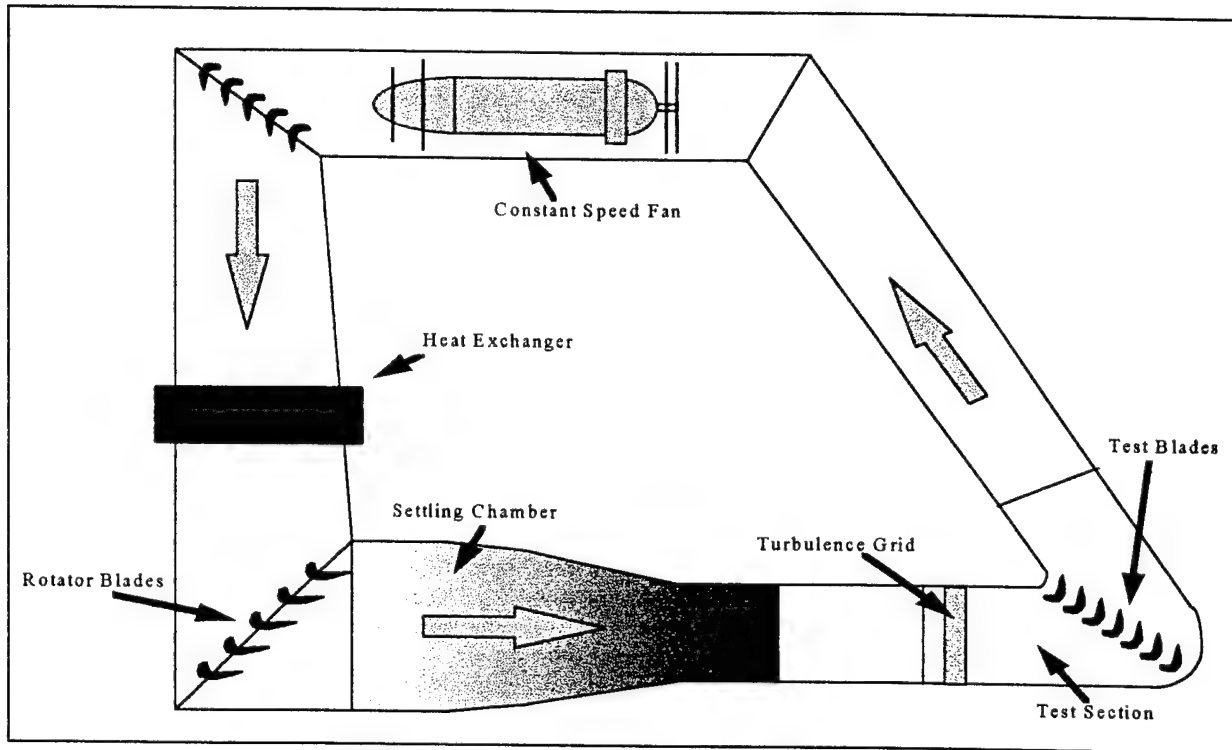


Figure 2: Cascade Wind Tunnel Schematic

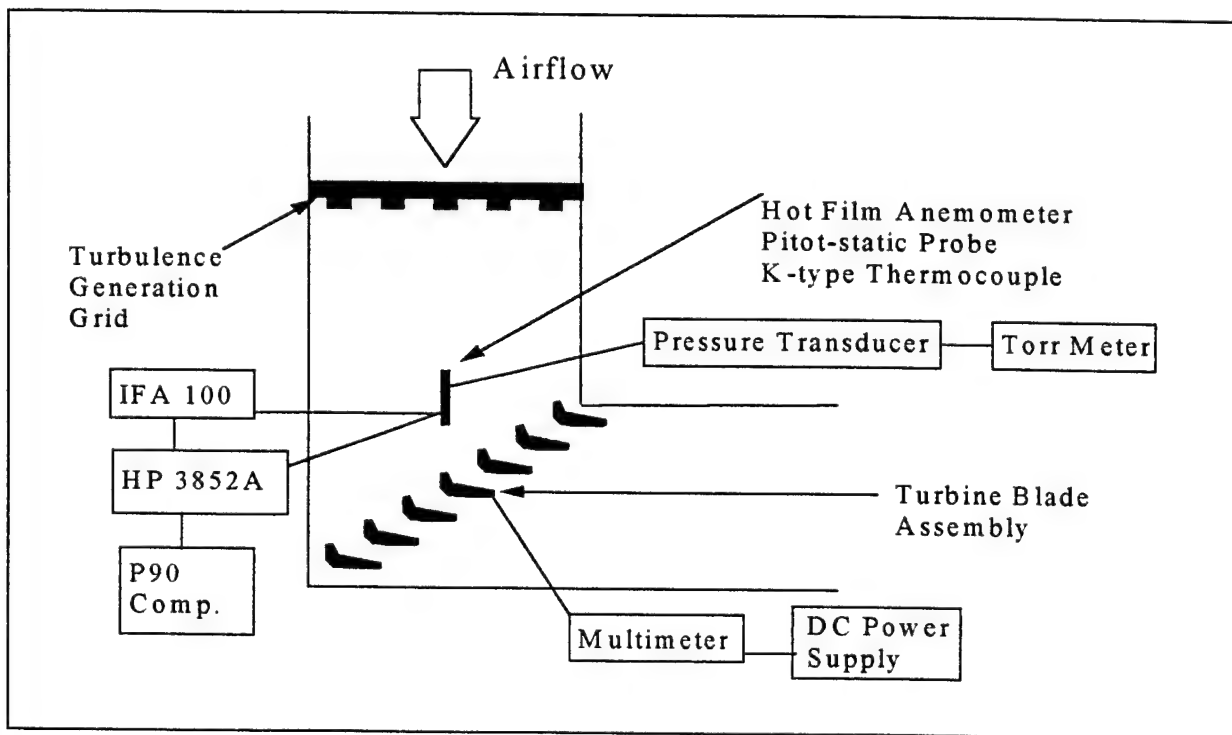


Figure 3: Test Section Diagram

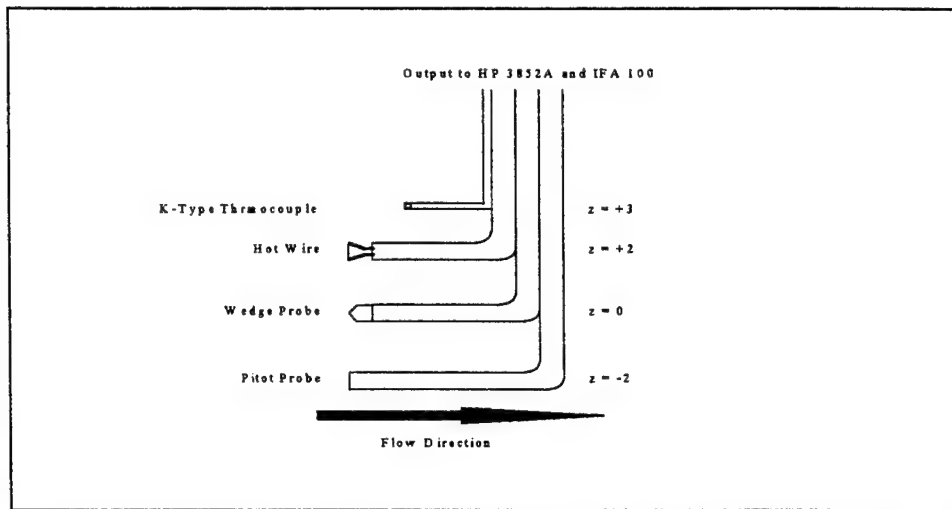


Figure 4: Traversable Test Probe

The setup for collecting heat transfer data centers on the test blade. The test blade is located in the center of the cascade. It is made of closed cell polystyrene, which is covered with Super 77 aerosol adhesive and a thin gold film with a resistance per square of 2.512 ohm/sq. This gold film is then covered with black paint and sprayed with 35W1 liquid crystals. The liquid crystals are active in the 35-36° Celsius range, with the yellow band indicating 35.7° Celsius. The gold acts as a conductor and provides resistance heating to the blade. Two electrodes at the trailing edge are connected to a DC power supply providing up to 5 amps. A multimeter is placed in series with the power supply and the blade to provide current readings. The entire test blade setup can be seen in Figure 4. This test blade allows for surface temperature a current readings to be taken which then allow heat transfer calculations to be performed.

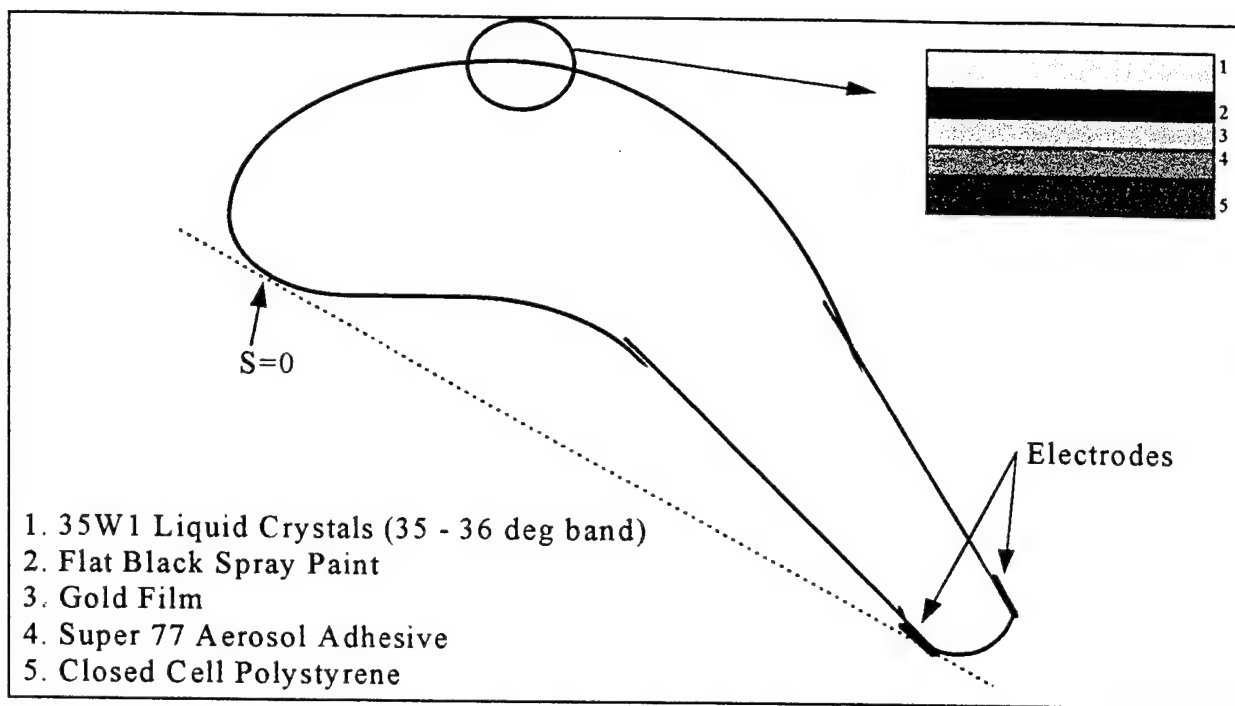


Figure 5: Test Blade Setup

The turbulence grids are constructed of square wood pieces which are nailed together in a square grid lattice. Two turbulence grids were constructed for this procedure, one grid of 1/2 in. diameter bars and one grid of 2 3/8 in. diameter bars.

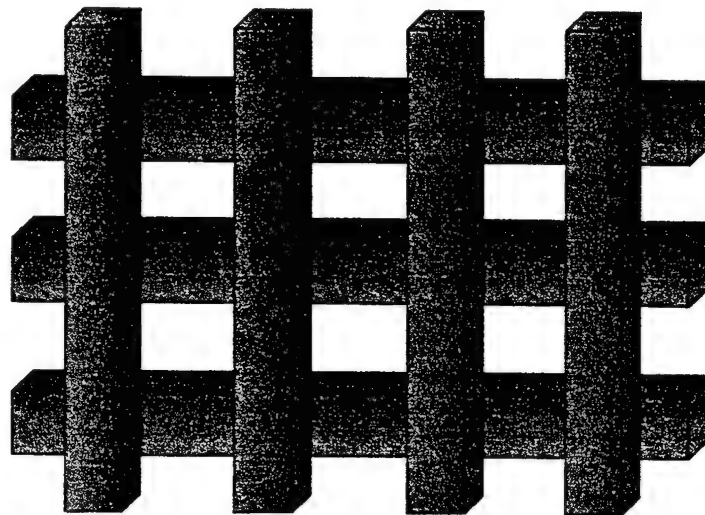


Figure 6: Grid of 2 3/8 in Diameter Bars

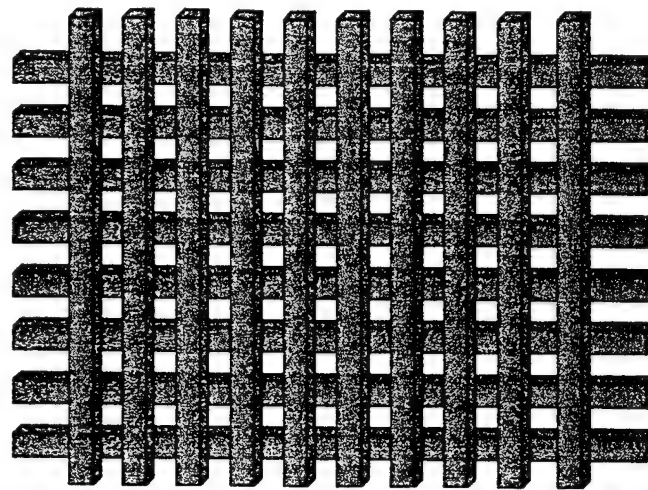


Figure 7: Grid of 1/2 in Diameter Bars

The full list of equipment used in this investigation is as follows:

Table of Equipment

Cascade Wind Tunnel, U.S. Air Force Academy Aeronautics Lab
 1/2 in. and 2 in. square mesh of square bars turbulence generation grids
 Pitot-static tube
 Pressure transducer
 Torr pressure gage, SN 54258-1
 Hot film anemometer, TSI Model 1210-20, SN 925113
 K type Thermocouples
 IFA 100 Intelligent Flow Analyzer
 HP 3852A data acquisition/control unit
 IBM compatible Pentium 90 computer
 TV3 Software
 SPSS Statistical Software
 Microsoft Excel 4.0 Software
 Styrofoam turbine blade assembly (See Figure 4)
 HP 6434B DC power supply
 Fluke 27/FM Multimeter

Table 1: List of Equipment

The instrument calibration for this experiment was already performed by laboratory personnel annually. The hot wire anemometer calibration is a fourth order curve fit which had been previously determined. The thermocouples, pressure transducers, thermometers and

barometers were calibrated by USAFA PMEL. The liquid crystals on the blade were also calibrated previously.

Experimental Procedure

To obtain turbulent heat transfer and flow data use the following procedure:

- a: Using a clean tunnel configuration place the hot wire portion of the test probe at the center line position in front of the test blade. Ensure that the hot wire is directly into the flow. Raise the hot wire to a vertical position in the center of the gold section, ($z = 9$ in.). With the probe located in this position take zero velocity data for the hot wire, pitot-static probe and temperature. Note the atmospheric pressure.
- b. Turn on the air allowing the tunnel to spool up to steady state (approximately 9 m/s). Then setting the TV3 software to take continuous data for 2.5 seconds at 6000 Hz on the hot wire, take hot wire, pitot-static and temperature data. Ensure that the temperature remains close to the zero velocity data. This data will be used to determine the integral length scale and turbulence intensity. In the same position set the TV3 to take continuous data at 15000 Hz for 1 second on the hot wire and take the same types of data. This data will be used to analyze the micro length scales and turbulence intensity. Note the turbulence intensity should be the same.
- c. Using the cooling flow, allow the tunnel to reach a steady state temperature of 25 Celsius. adjust the cooling flow to ensure that this temperature is maintained.
- d. When the tunnel has reached steady state carefully apply current from the power source to the test blade until the liquid crystals become active. When the liquid crystals are active note the position of the yellow band on both the suction and pressure sides as well as the current being applied. By gently adjusting the current, the yellow band can be moved over the entire blade

noting the position and current at each position on the blade. Note any indications of flow phenomenon such as transition and Taylor-Görtler vortices. Use care not to overload the blade as it could cause the foam core to melt and ruin the test blade.

- e. Place the 2 3/8 in grid in the wind tunnel at the previously calculated distance for 10% turbulence intensity (approximately 72 in.). This is as far back from the blade as the test section allows. Take zero velocity and turbulent flow data as described above. Using SPSS analyze the continuous data to determine the turbulence intensity.
- f. Move the data probe out of the flow and adjust the position of the grid forward to account for the distance between the probe and the turbine blade so that the blade itself is now seeing 10% turbulence intensity.
- g. Run the tunnel up to steady state as describe for the clean tunnel case and take heat transfer data using the same procedure described in the clean tunnel case.
- h. Replace the 2 3/8 in. turbulence generation grid with the 1/2 in. turbulence generation grid and repeat the same procedure used for the 2 3/8 in. grid. Take turbulence data and move the grid as necessary to match the large grid turbulence intensity.
- i. Reduce all data for all flows and heat transfer to determine any possible relationship between length scales and heat transfer.

Uncertainty Analysis

The uncertainty analysis of the heat transfer data was performed using the Kline-McClintock method. The equations of interest here are as follows:

$$q'' = \frac{I^2 R_{35.7}}{w^2} \quad [12]$$

$$\hat{q}_c = \hat{q} - \varepsilon\sigma(T_{LC}^4 - T_\infty^4) - \hat{q}_L \quad [13]$$

$$h = \frac{\hat{q}_c}{(T_{LC} - T_\infty)} \quad [14]$$

The equations were then placed in an Excel 4.0 spreadsheet along with the uncertainty equations in order to determine the expected uncertainty. Since our current ranges from 2.0 amps to 5.0 amps, the calculated uncertainty as per the spreadsheet in h ranges from 9.01% at 2.0 amps to 5.64% at 5.0 amps. This is well within acceptable parameters for this type of experiment. This spreadsheet is shown below in Figure 5.

			% Uncertainty	\hat{q}' Uncertainty	% \hat{q}'' Uncertainty	\hat{q}''' Uncertainty	% \hat{q}''' Uncertainty	h Uncertainty	% h Uncertainty
Current	5.00 +/- 0.0050 Amps		0.10	3.01	0.20	3.01	0.21	0.28	0.21
Resistance	2.51 +/- 0.1256 Ohms/sq		5.00	75.31	5.00	75.31	5.20	7.04	5.20
Film Width	0.20 +/- 0.0002 m		0.10	-2.93	-0.19	-2.93	-0.20	-0.27	-0.20
Tinf	25.00 +/- 0.1500 deg C		0.60	Not Used	Not Used	0.77	0.05	1.97	1.45
TLC	35.70 +/- 0.1500 deg C		0.42	Not Used	Not Used	-0.85	-0.06	-1.98	-1.46
Emissivity	0.85 +/- 0.1500		17.65	Not Used	Not Used	-10.16	-0.70	-0.96	-0.70
Conduction	0.00 +/- 0.0000 W/m^2		0.00	Not Used	Not Used	0.00	0.00	0.00	0.00
S-B Const	5.67E-08 W(m^2K^4)								
$\hat{q}' =$	1506.219 +/- 75.428 W/m^2		5.01 % Uncertainty						
$\hat{q}''' =$	1448.624 +/- 76.118 W/m^2		5.25 % Uncertainty						
$h =$	135.385 +/- 7.641 W(m^2K)		5.64 % Uncertainty						

Figure 8: Uncertainty Analysis

Results and Discussion

The results and discussion will be presented in three separate sections for each of the cascade tunnel configurations (clean, $\frac{1}{2}$ in. grid, $2\frac{3}{8}$ in grid). After each configuration is presented and discussed and overall evaluation and discussion of the experiment will be presented.

“Clean” Tunnel Configuration (No Turbulence Grid)

The turbulence data for all runs was taken at the center of the tunnel with the hot film anemometer aligned with the center of the test blade. All data is taken at this point over time. The key flow information for the clean tunnel run is tabulated below:

Flow Information	
Atmospheric Pressure	11.183 psia
Hot Film Zero Voltage	-5.351 V
Torr Meter Delta P	0.280 Torr
Mean Velocity	8.807 m/s @ 6000 Hz 8.799 m/s @ 15000 Hz
Standard Deviation	0.044 m/s @ 6000 Hz 0.040 m/s @ 15000 Hz
Turbulence Intensity	0.50% @ 6000 Hz
Micro-Length Scale	Infinite
Integral Length Scale	0.00543 m @ 15000 Hz 0.214 in @ 15000 Hz

Table 2: Clean Tunnel Flow Information

With this turbulence data taken, the heat transfer data was then taken and reduced. This data provided a baseline from which the effects of the turbulence could later be determined. This data was plotted against data provided by Capt Butler which was taken last semester. The data agreed nicely with last semester’s data in all points but the stagnation point, which appeared to be high on our run. Since this is an important point and there was significant fluctuation in temperature during the test run, it was decided to retest this point at several temperatures. This would determine whether there was a temperature dependency that was not removed by the data reduction or whether this was just an errant point. The results of the stagnation collection are shown below. The stagnation data points were relatively flat when retaken vs. temperature and all variation was within our experimental error. This supports the previous expectations. The average of these points was then entered as the stagnation heat transfer.

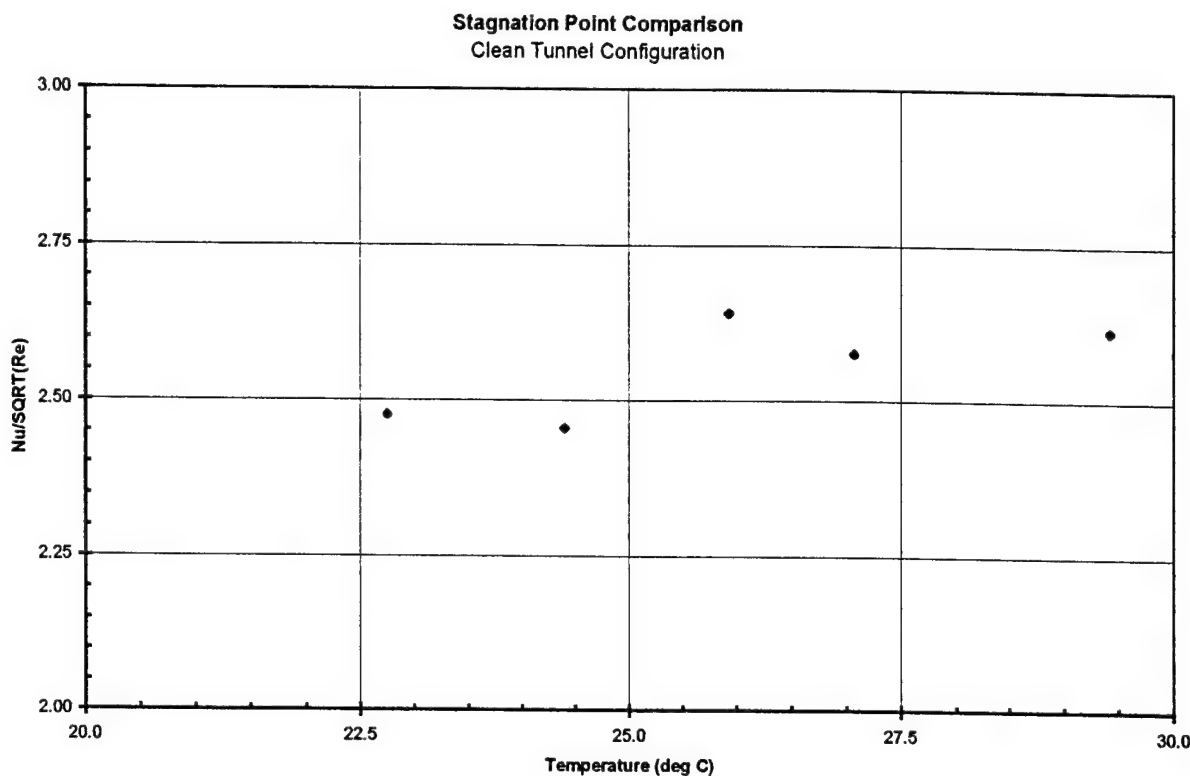


Figure 9: Stagnation Point Comparison

With the new stagnation point all the data for the clean tunnel lined up within the expected error and provided confidence in the data gathering technique. Some significant observations included an area on both the pressure side and the suction side where the foil had bubbled at the midspan of the blade. This bubbling caused flow irregularities such as separation and premature transition of the boundary layer. To account for this the data was taken from the top portion of the blade which was unaffected by these irregularities. While this does not necessarily invalidate the data it could be a source of error that later studies must consider.

Also of interest was the formation of spanwise variations on the pressure side of the blade that could represent Taylor-Görtler vortices. This is represented on the plot by the range of data points for a given Nusselt number.

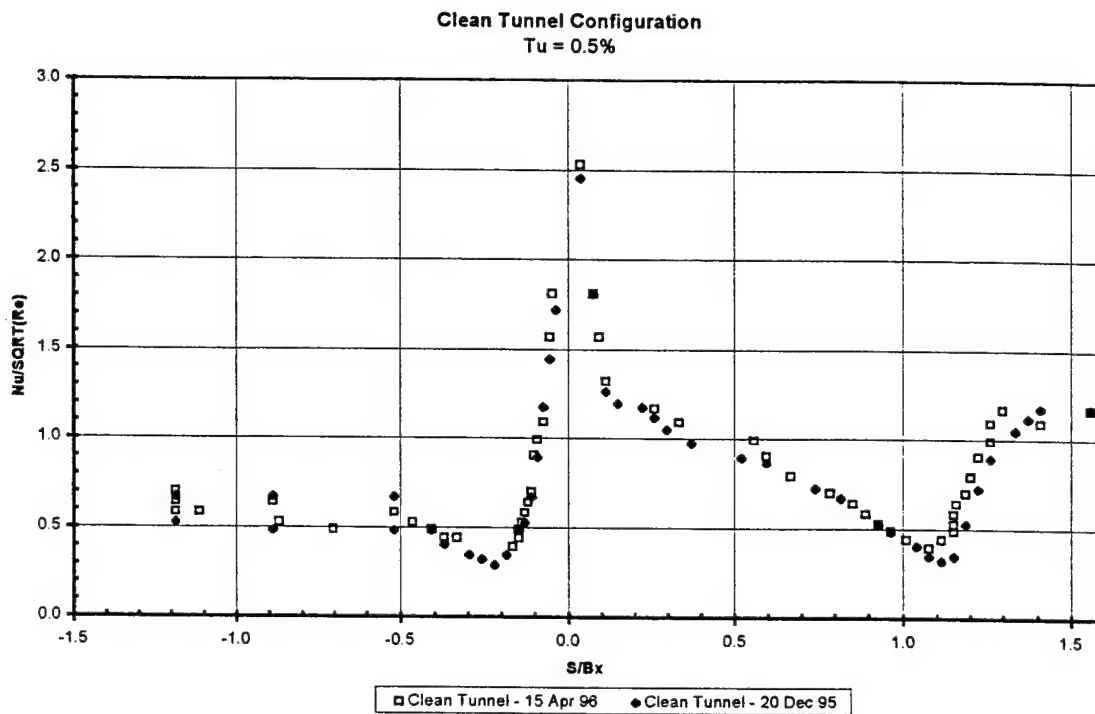


Figure 10: Clean Tunnel Comparison

2 3/8 in Grid Configuration

With the 2 3/8 in diameter bar turbulence grid in the test section, the turbulent flow data was reduced to give the following flow information.

Flow Information	
Atmospheric Pressure	11.216 psia
Hot Film Zero Voltage	-5.36 V
Torr Meter Delta P	0.276 Torr
Mean Velocity	8.882 m/s @ 6000 Hz 8.658 m/s @ 15000 Hz
Standard Deviation	0.831 m/s @ 6000 Hz 0.881 m/s @ 15000 Hz
Turbulence Intensity	10.18% @ 6000 Hz
Micro-Length Scale	0.07053 m @ 6000 Hz 2.777 in @ 6000 Hz
Integral Length Scale	0.00837 m @ 15000 Hz 0.330 in @ 15000 Hz

Table 3: 2 3/8 in Grid Flow Information

This flow represents high turbulence intensity with large length scales and as expected affected the turbulence intensity by moving the transition point forward on the blade, and increasing heat transfer. The transition points moved forward 0.1875 in on the pressure side and 0.625 in on the suction side. At the stagnation point the heat transfer was increased by 6.25%. The spanwise distribution on the pressure side disappeared and post-transition heat transfer on the pressure side was dramatically increased by as much as 52 %. Elsewhere, increases in heat transfer were more moderate, on the order of the stagnation point increases. This distribution is shown in Figure 11.

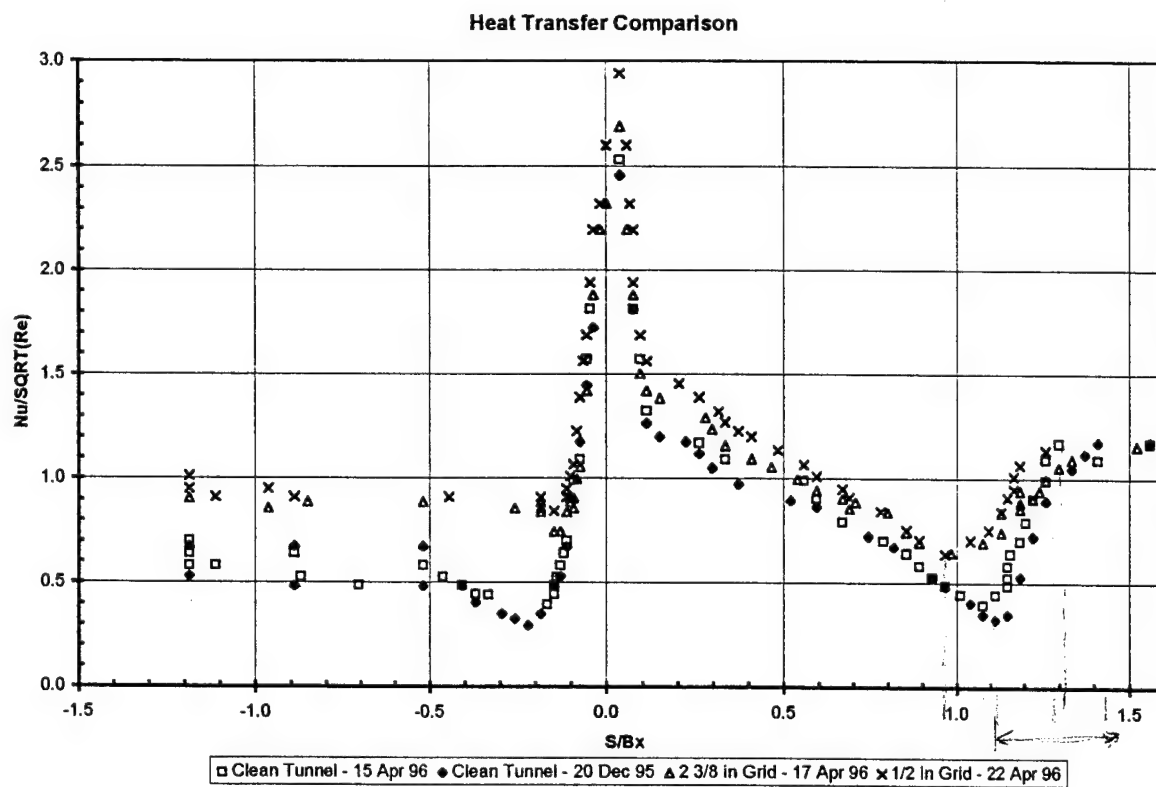


Figure 11: Heat Transfer Comparison

1/2 in Grid Configuration

With the 1/2 in turbulence grid in place the flow data was reduced to give the following flow information:

Flow Information	
Atmospheric Pressure	11.216 psia
Hot Film Zero Voltage	-5.34 V
Torr Meter Delta P	0..301 Torr
Mean Velocity	9.347 m/s @ 6000 Hz 8.998 m/s @ 15000 Hz
Standard Deviation	0.949 m/s @ 6000 Hz 0.894 m/s @ 15000 Hz
Turbulence Intensity	10.15% @ 6000 Hz
Micro-Length Scale	0.01320 m @ 6000 Hz 0.520 in @ 6000 Hz
Integral Length Scale	0.00490 m @ 15000 Hz 0.193 in @ 15000 Hz

Table 4: 1/2 in Grid Flow Information

The heat transfer data for this run, also plotted in Figure 11, shows the same trends as the 2 3/8 in grid. This is expected due to the nearly identical turbulence intensity. With this grid, however, the length scales are much smaller. The 1/2 in grid produced higher heat transfer rates than the 2 3/8 in grid until transition, which occurred at the same points as with the large grid. After transition the heat transfer characteristics were the same as the large grid characteristics. At stagnation the heat transfer was 16.2% higher than the clean tunnel and 9.4% higher than that produced by the large grid. Similarly the other data points before transition were higher than both the large grid and clean tunnel. Since this difference is greater than our uncertainty this represents a significant finding on the affect of length scales on heat transfer. The differences between the two grids are better highlighted in Figure 12 where just those two data sets are plotted. Additionally, lines are added to highlight the differences.

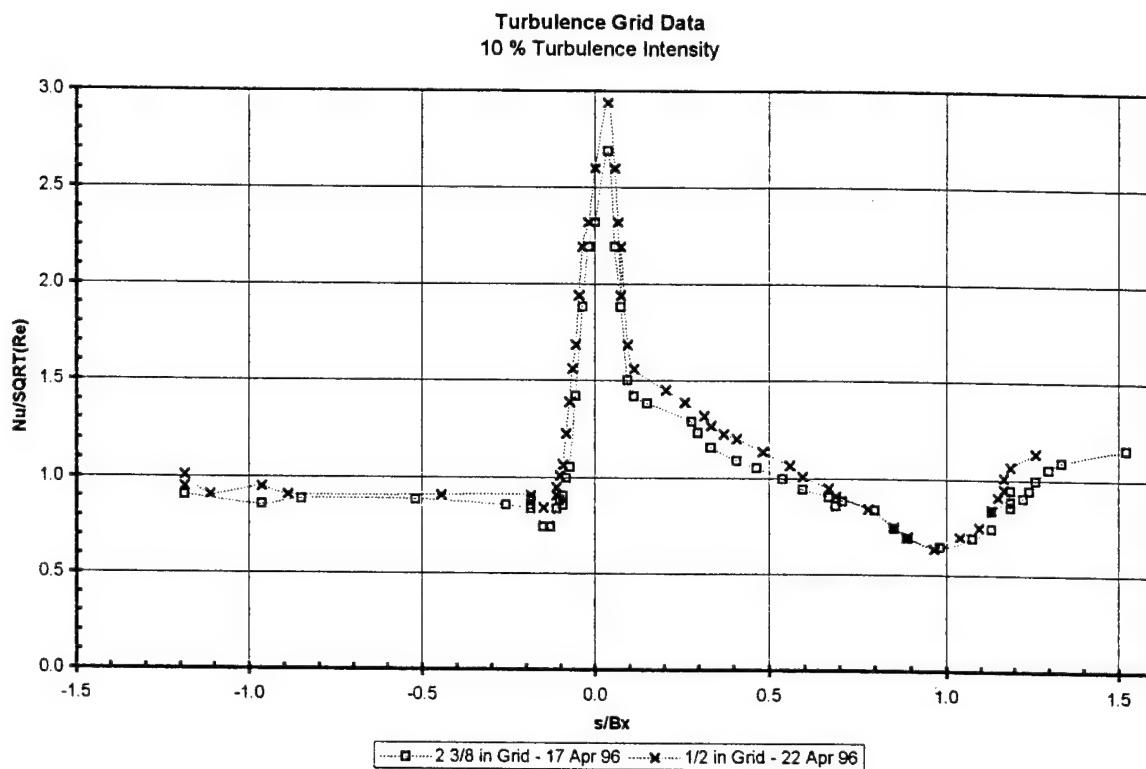


Figure 12: Grid Comparison

Overall Discussion

The heat transfer characteristics of the turbine blade responded to turbulence intensity in the same manner as had already been shown by previous work such as Baughn et al. The effects of length scales appear to be primarily in the region of pre-transition heat transfer. The transition points are unaffected by the length scales, but a shorter length scale appears to cause a significant increase in heat transfer at the same turbulence intensity. This increase lasts until boundary layer transition where the free-stream turbulence become insignificant compared to the turbulent boundary layer.

Conclusions

The effects of operating a turbine blade under high turbulence intensity, such as the 10.15% to 10.18% used in this investigation are an increase in heat transfer over the entire blade, the boundary layer transition points move forward on both blade surfaces, and the disappearance of spanwise heat transfer variations on the pressure side. In addition to these documented effects, it appears that smaller length scales at the same turbulence intensity produces higher heat transfer than that produced by longer length scales. In this test the stagnation temperature produced by the 1/2 in grid was 9% higher than that produced by the 2 3/8 in grid. The length scales appear to have no effect on transition location and the effects of differing length scales disappear after boundary layer transition. This is most likely due to the relative insignificance of the free-stream turbulence compared to the boundary layer turbulence. This investigation shows that length scales therefore have a significant impact on pre-transition heat transfer in turbine blades.

Recommendations

The investigation of the effects of length scales on heat transfer should be continued. Tests should be conducted at different turbulence intensity levels and with more gradations of length scale in order to try and quantify the effect of length scales on the turbine heat transfer. Improvements on this experiment would be to include a better blade so that data can be taken over the entire blade. Also the people taking data could be more familiar with liquid crystals to allow for better readings of the crystals. Where possible have the same points measured by the same person in order to eliminate error introduced by having different people view the crystals. A greater understanding of length scales is essential to understanding turbulent heat transfer, especially since this investigation has shown that they have a significant impact on heat transfer.

Acknowledgments

We would like to acknowledge our sponsors, LtCol Barlow, LtCol Van Treuren, and Capt Butler, for their patient instruction and support for this project. Also we give thanks to SSgt Evans for providing facility support.

References

Baughn, James W., and Robert J. Butler, Aaron R. Byerley, and Richard B. Rivir, "An Experimental Investigation of Heat Transfer, Transition and Separation on Turbine Blades at Low Reynolds Number and High Turbulence Intensity," *ASME International Engineering Congress & Exposition*, San Francisco, CA, 1995.

Duncan, John, and Kristen Peterson, "AE 471 Aero-thermal Cascade Tunnel Flow Quality: Turbulence Generation and Prediction," Department of Aeronautics, USAF Academy, CO, 1995.

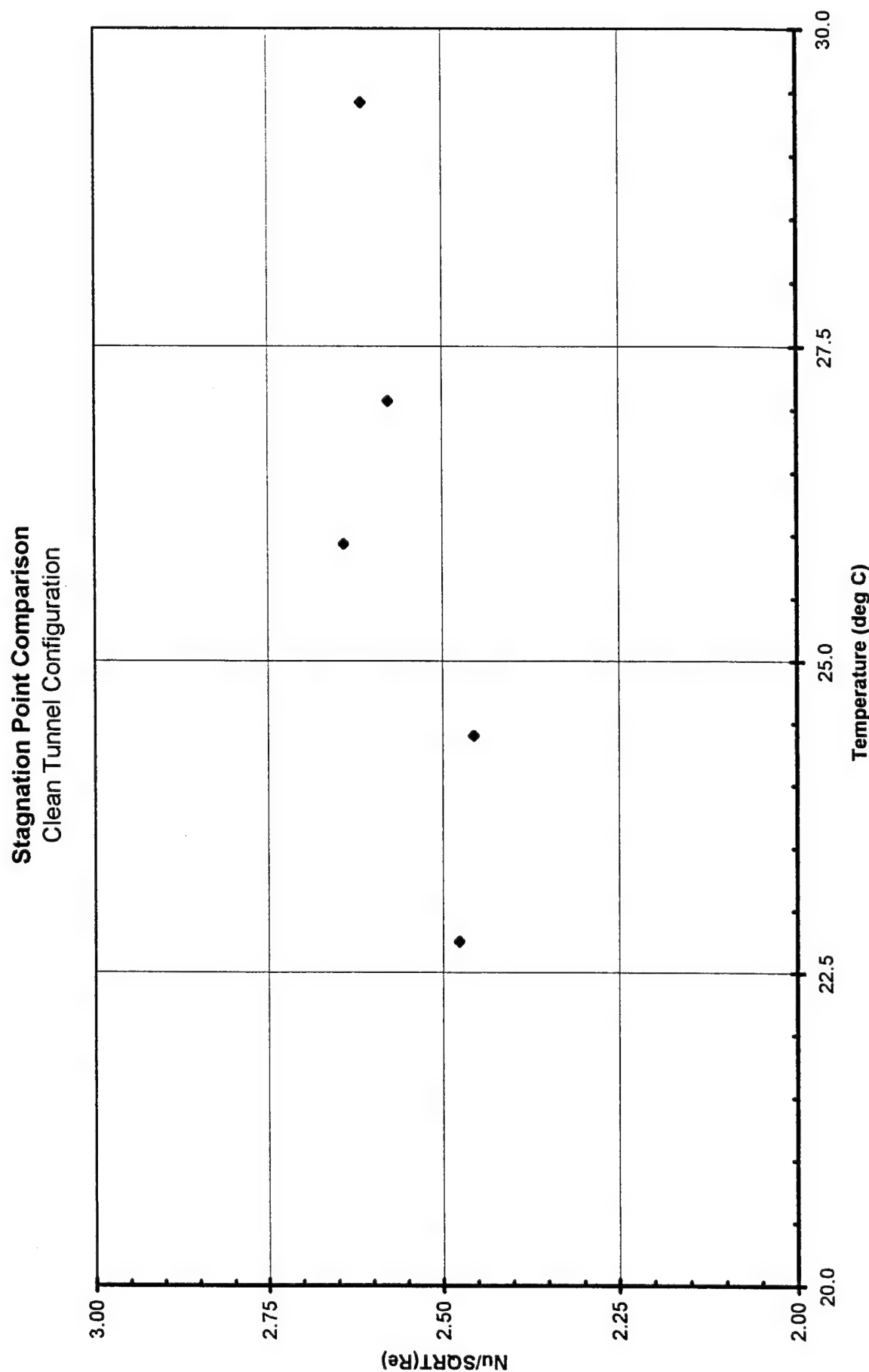
Incropera, Frank P., and David P. De Witt, *Fundamentals of Heat and Mass Transfer*, 3rd. Ed., John Wiley & Sons, New York, NY, 1990.

Langston, L. S., M. L. Nice, and R. M. Hooper, "Three-Dimensional Flow Within a Turbine Cascade Passage," *Journal of Engineering for Power*, January 1997, pp. 21-28.

Roach, P. E., "The Generation of Nearly Isotropic Turbulence by Means of Grids," *Heat and Fluid Flow*, Vol. 8, No. 2, June 1987, pp. 82-92.

VanFossen, G. James Jr., and Robert J. Simoneau, "Preliminary Results of a Study of the Relationship Between Free Stream Turbulence and Stagnation Region Heat Transfer," *NASA Technical Memorandum*, No. 86884

Appendix A: Heat Transfer Graphs

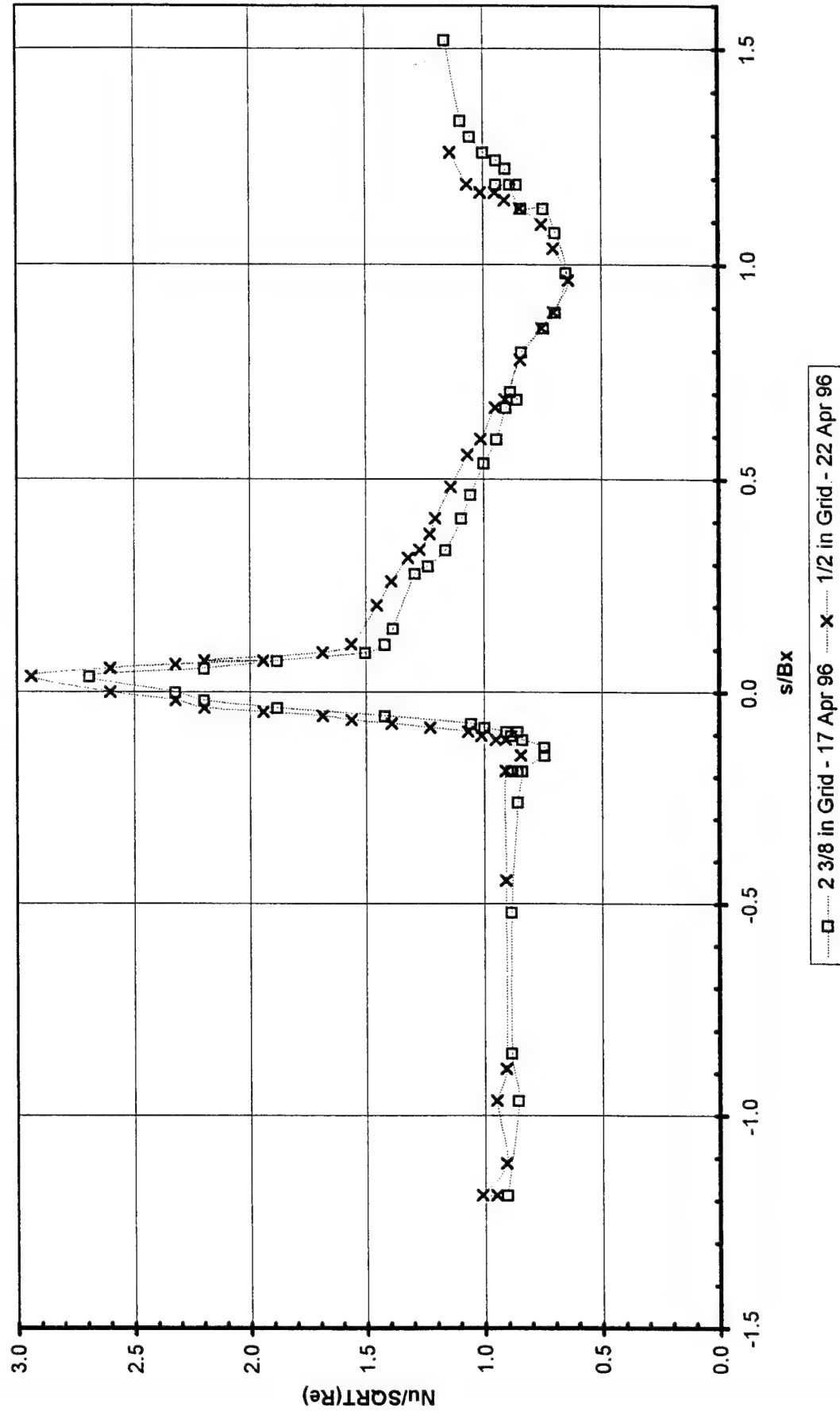


B1

Clean Tunnel - 20 Dec 95

P inf =	11.311	psi		Rho =	0.9137	kg/m^3			
T inf =	24.400	C		Mu =	1.8337E-05	N s/m^2			
T lc =	35.700	C		k air =	0.0261	W/mK			
Delta P =	0.291	torr		V inf =	9.215	m/s			
L =	18.531	in		Bx =	6.740	in			
W =	8.039	in		Re =	78610.3				
R" =	2.512	Ohms/SQ		Cond. =	0	W/m^2			
Emmis. =	0.850			S-B Con. =	5.670E-08	W/m^2K^4			
Clean Tunnel Configuration - Clean Tunnel - 20 Dec 95									
s (in)	s/Bx	Current (Amps)	T inf (C)	q" (W/m^2)	qc" (W/m^2)	h (W/m^2K)	St	Nu	Nu/SQRT(Re)
-8.000	-1.1869	2.29	24.4	315.951	255.304	22.593	0.002665	148.152	0.5284
-8.000	-1.1869	2.53	24.4	385.646	325.000	28.761	0.003392	188.596	0.6727
-6.000	-0.8902	2.21	24.4	294.261	233.615	20.674	0.002438	135.565	0.4835
-6.000	-0.8902	2.53	24.4	385.646	325.000	28.761	0.003392	188.596	0.6727
-3.500	-0.5193	2.21	24.4	294.261	233.615	20.674	0.002438	135.565	0.4835
-3.500	-0.5193	2.53	24.4	385.646	325.000	28.761	0.003392	188.596	0.6727
-2.750	-0.4080	2.21	24.4	294.261	233.615	20.674	0.002438	135.565	0.4835
-2.500	-0.3709	2.06	24.4	255.672	195.025	17.259	0.002036	113.172	0.4036
-2.000	-0.2967	1.95	24.4	229.096	168.450	14.907	0.001758	97.750	0.3486
-1.750	-0.2596	1.90	24.4	217.498	156.852	13.881	0.001637	91.020	0.3246
-1.500	-0.2226	1.83	24.4	201.767	141.121	12.489	0.001473	81.892	0.2921
-1.250	-0.1855	1.95	24.4	229.096	168.450	14.907	0.001758	97.750	0.3486
-1.000	-0.1484	2.21	24.4	294.261	233.615	20.674	0.002438	135.565	0.4835
-0.875	-0.1298	2.29	24.4	315.951	255.304	22.593	0.002665	148.152	0.5284
-0.750	-0.1113	2.53	24.4	385.646	325.000	28.761	0.003392	188.596	0.6727
-0.625	-0.0927	2.86	24.4	492.811	432.164	38.245	0.004511	250.783	0.8945
-0.500	-0.0742	3.23	24.4	628.569	567.923	50.259	0.005928	329.562	1.1754
-0.375	-0.0556	3.55	24.4	759.285	698.639	61.826	0.007292	405.416	1.4460
-0.250	-0.0371	3.85	24.4	893.037	832.391	73.663	0.008688	483.032	1.7228
0.250	0.0371	4.55	24.4	1247.300	1186.654	105.014	0.012385	688.608	2.4560
0.500	0.0742	3.94	24.4	935.278	874.631	77.401	0.009129	507.544	1.8102
0.750	0.1113	3.34	24.4	672.111	611.465	54.112	0.006382	354.829	1.2656
1.000	0.1484	3.26	24.4	640.300	579.653	51.297	0.006050	336.370	1.1997
1.500	0.2226	3.23	24.4	628.569	567.923	50.259	0.005928	329.562	1.1754
1.750	0.2596	3.16	24.4	601.620	540.974	47.874	0.005646	313.924	1.1197
2.000	0.2967	3.07	24.4	567.839	507.192	44.884	0.005294	294.321	1.0497
2.500	0.3709	2.97	24.4	531.448	470.802	41.664	0.004914	273.204	0.9744
3.500	0.5193	2.86	24.4	492.811	432.164	38.245	0.004511	250.783	0.8945
4.000	0.5935	2.82	24.4	479.122	418.476	37.033	0.004368	242.839	0.8661
5.000	0.7418	2.61	24.4	410.421	349.774	30.953	0.003651	202.972	0.7239
5.500	0.8160	2.53	24.4	385.646	325.000	28.761	0.003392	188.596	0.6727
6.250	0.9273	2.29	24.4	315.951	255.304	22.593	0.002665	148.152	0.5284
6.500	0.9644	2.21	24.4	294.261	233.615	20.674	0.002438	135.565	0.4835
7.000	1.0386	2.06	24.4	255.672	195.025	17.259	0.002036	113.172	0.4036
7.250	1.0757	1.95	24.4	229.096	168.450	14.907	0.001758	97.750	0.3486
7.500	1.1128	1.90	24.4	217.498	156.852	13.881	0.001637	91.020	0.3246
7.750	1.1499	1.95	24.4	229.096	168.450	14.907	0.001758	97.750	0.3486
8.000	1.1869	2.29	24.4	315.951	255.304	22.593	0.002665	148.152	0.5284
8.250	1.2240	2.61	24.4	410.421	349.774	30.953	0.003651	202.972	0.7239
8.500	1.2611	2.86	24.4	492.811	432.164	38.245	0.004511	250.783	0.8945
9.000	1.3353	3.07	24.4	567.839	507.192	44.884	0.005294	294.321	1.0497
9.250	1.3724	3.16	24.4	601.620	540.974	47.874	0.005646	313.924	1.1197
9.500	1.4095	3.23	24.4	628.569	567.923	50.259	0.005928	329.562	1.1754
10.500	1.5579	3.23	24.4	628.569	567.923	50.259	0.005928	329.562	1.1754

Turbulence Grid Data
10 % Turbulence Intensity



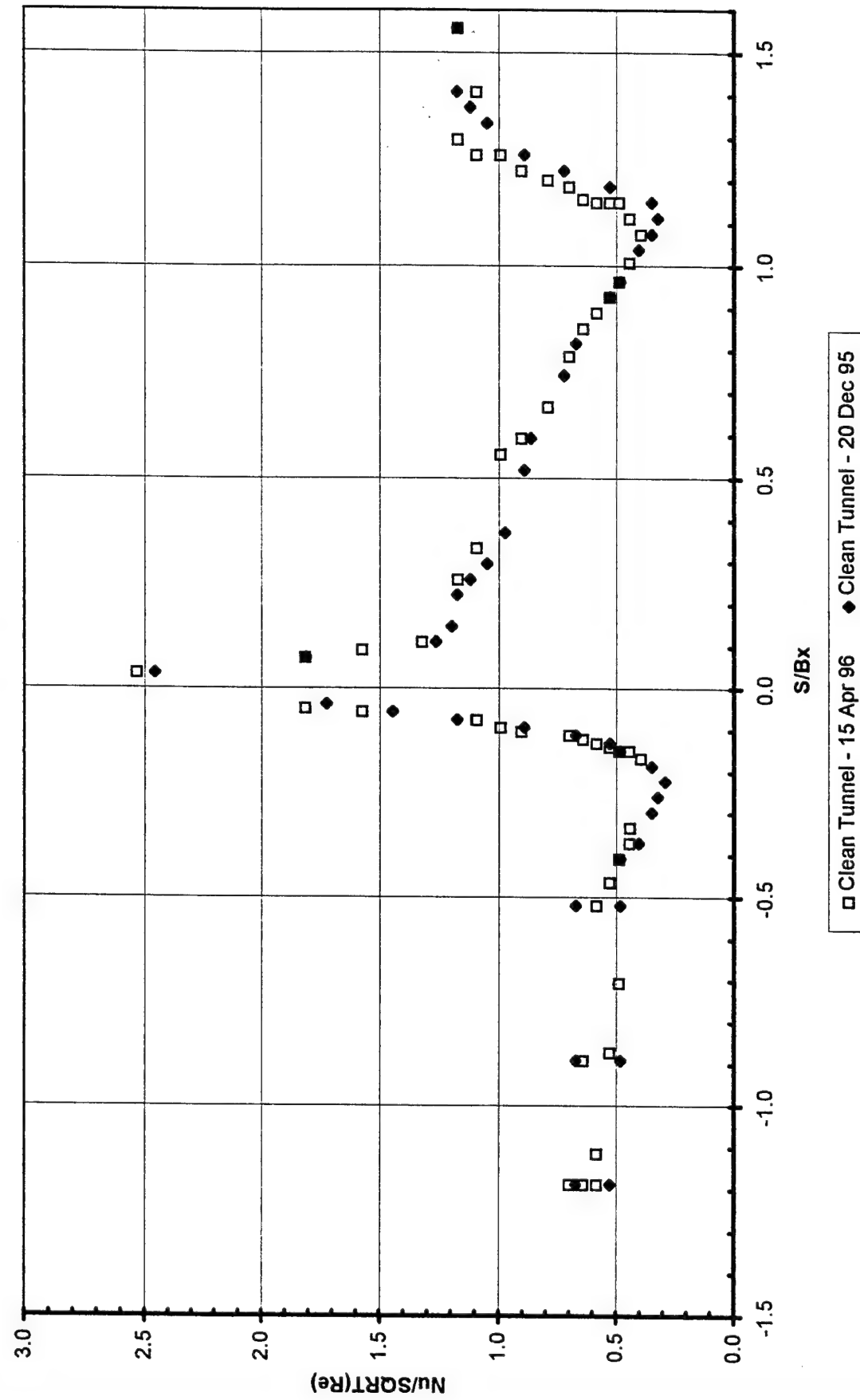
P inf =	11.216	psi	Rho =	0.9039	kg/m^3				
T inf =	25.100	C	Mu =	1.837E-05	N s/m^2				
T lc =	35.700	C	K air =	0.0262	W/mK				
Delta P =	0.276	torr	V inf =	9.023	m/s				
L =	18.531	in	Bx =	6.740	in				
W =	8.039	in	Re =	76007.9					
R" =	2.512	Ohms/SQ	Cond. =	0	W/m^2				
Emiss. =	0.850		S-B Con. =	5.670E-08	W/m^2K^4				
<hr/>									
2 3/8 in. Grid at 72 3/4 in. -			2 3/8 in Grid - 17 Apr 96						
s (in)	s/Bx	Current (Amps)	T inf (C)	q" (W/m^2)	qc" (W/m^2)	h (W/m^2K)	St	Nu	Nu/SQRT(Re)
-8.000	-1.1869	2.79	25.0	467.303	409.504	38.129	0.004642	249.528	0.9051
-6.500	-0.9644	2.73	24.9	447.385	389.382	36.121	0.004398	236.387	0.8574
-5.750	-0.8531	2.70	25.4	439.213	383.817	37.373	0.004550	244.579	0.8871
-3.500	-0.5193	2.70	25.4	439.213	383.817	37.373	0.004550	244.579	0.8871
-1.750	-0.2596	2.73	24.9	447.385	389.382	36.121	0.004398	236.387	0.8574
-1.250	-0.1855	2.64	25.4	419.910	364.308	35.335	0.004302	231.247	0.8388
-1.250	-0.1855	2.70	25.4	439.213	383.817	37.373	0.004550	244.579	0.8871
-1.250	-0.1855	2.73	24.9	447.385	389.382	36.121	0.004398	236.387	0.8574
-1.000	-0.1484	2.52	25.3	382.604	326.439	31.328	0.003814	205.022	0.7437
-0.875	-0.1298	2.52	25.3	382.604	326.439	31.328	0.003814	205.022	0.7437
-0.750	-0.1113	2.64	25.4	419.910	364.308	35.335	0.004302	231.247	0.8388
-0.688	-0.1020	2.70	25.4	439.213	383.817	37.373	0.004550	244.579	0.8871
-0.625	-0.0927	2.73	24.9	447.385	389.382	36.121	0.004398	236.387	0.8574
-0.625	-0.0927	2.79	25.0	467.303	409.504	38.129	0.004642	249.528	0.9051
-0.563	-0.0835	2.91	24.9	510.193	452.292	42.035	0.005118	275.088	0.9978
-0.500	-0.0742	2.98	25.0	535.033	477.183	44.389	0.005405	290.498	1.0537
-0.375	-0.0556	3.38	25.1	688.306	631.375	59.733	0.007273	390.911	1.4179
-0.250	-0.0371	3.85	25.2	893.037	836.208	79.261	0.009651	518.714	1.8815
-0.125	-0.0185	4.14	25.2	1032.640	975.811	92.494	0.011262	605.312	2.1956
0.000	0.0000	4.25	25.2	1085.684	1029.009	97.815	0.011910	640.131	2.3219
0.250	0.0371	4.64	24.8	1297.132	1238.365	113.300	0.013795	741.471	2.6895
0.375	0.0556	4.14	25.2	1032.640	975.811	92.494	0.011262	605.312	2.1956
0.500	0.0742	3.85	25.2	893.037	836.208	79.261	0.009651	518.714	1.8815
0.625	0.0927	3.47	25.1	725.449	668.518	63.247	0.007701	413.908	1.5013
0.750	0.1113	3.38	25.1	688.306	631.375	59.733	0.007273	390.911	1.4179
1.000	0.1484	3.35	25.1	674.125	617.092	58.271	0.007095	381.346	1.3832
1.875	0.2782	3.25	25.1	636.378	579.038	54.370	0.006620	355.814	1.2906
2.000	0.2967	3.18	25.1	609.260	552.073	51.984	0.006329	340.203	1.2340
2.250	0.3338	3.11	24.9	582.732	524.831	48.776	0.005939	319.208	1.1578
2.750	0.4080	3.04	24.9	554.965	496.911	46.053	0.005607	301.386	1.0932
3.125	0.4636	2.98	25.0	535.033	477.183	44.389	0.005405	290.498	1.0537
3.625	0.5378	2.91	24.9	510.193	452.292	42.035	0.005118	275.088	0.9978
4.000	0.5935	2.85	24.9	487.655	429.550	39.773	0.004843	260.289	0.9441
4.500	0.6677	2.79	25.0	467.303	409.504	38.129	0.004642	249.528	0.9051
4.625	0.6862	2.73	24.9	447.385	389.382	36.121	0.004398	236.387	0.8574
4.750	0.7047	2.70	25.4	439.213	383.817	37.373	0.004550	244.579	0.8871
5.375	0.7975	2.64	25.4	419.910	364.308	35.335	0.004302	231.247	0.8388
5.750	0.8531	2.52	25.3	382.604	326.439	31.328	0.003814	205.022	0.7437
6.000	0.8902	2.45	25.3	361.643	305.428	29.284	0.003566	191.642	0.6951
6.625	0.9829	2.37	25.3	338.411	282.554	27.274	0.003321	178.487	0.6474
7.250	1.0757	2.45	25.3	361.643	305.428	29.284	0.003566	191.642	0.6951
7.625	1.1313	2.52	25.3	382.604	326.439	31.328	0.003814	205.022	0.7437
7.625	1.1313	2.64	25.4	419.910	364.308	35.335	0.004302	231.247	0.8388
8.000	1.1869	2.70	25.4	439.213	383.817	37.373	0.004550	244.579	0.8871
8.000	1.1869	2.73	24.9	447.385	389.382	36.121	0.004398	236.387	0.8574
8.000	1.1869	2.85	24.9	487.655	429.550	39.773	0.004843	260.289	0.9441
8.250	1.2240	2.79	25.0	467.303	409.504	38.129	0.004642	249.528	0.9051
8.375	1.2426	2.85	24.9	487.655	429.550	39.773	0.004843	260.289	0.9441
8.500	1.2611	2.91	24.9	510.193	452.292	42.035	0.005118	275.088	0.9978
8.750	1.2982	2.98	25.0	535.033	477.183	44.389	0.005405	290.498	1.0537
9.000	1.3353	3.04	24.9	554.965	496.911	46.053	0.005607	301.386	1.0932
10.250	1.5208	3.11	24.9	582.732	524.831	48.776	0.005939	319.208	1.1578

P inf =	11.396	psi	Rho =	0.9179	kg/m^3			
T inf =	25.250	C	Mu =	1.8377E-05	N s/m^2			
T lc =	35.700	C	K air =	0.0262	W/mK			
Delta P =	0.277	torr	V inf =	8.970	m/s			
L =	18.531	in	Bx =	6.740	in			
W =	8.039	in	Re =	76705.1				
R" =	2.512	Ohms/SQ	Cond. =	0	W/m^2			
Emmis. =	0.850		S-B Con. =	5.670E-08	W/m^2K^4			

Clean Tunnel Configuration -		Clean Tunnel - 15 Apr 96							
s (in)	s/Bx	Current (Amps)	T inf (C)	q" (W/m^2)	qc" (W/m^2)	h (W/m^2K)	St	Nu	Nu/SQRT(Re)
-8.000	-1.1869	2.36	24.5	335.562	275.575	24.671	0.002975	161.387	0.5827
-8.000	-1.1869	2.45	24.6	361.643	301.809	27.092	0.003267	177.226	0.6399
-8.000	-1.1869	2.53	24.7	385.646	326.523	29.684	0.003580	194.179	0.7011
-7.500	-1.1128	2.36	24.5	335.562	275.575	24.671	0.002975	161.387	0.5827
-6.000	-0.8902	2.45	24.6	361.643	301.809	27.092	0.003267	177.226	0.6399
-5.875	-0.8717	2.27	24.5	310.456	250.317	22.350	0.002695	146.202	0.5279
-4.750	-0.7047	2.20	24.5	291.604	231.414	20.644	0.002490	135.041	0.4876
-3.500	-0.5193	2.36	24.5	335.562	275.575	24.671	0.002975	161.387	0.5827
-3.125	-0.4636	2.27	24.5	310.456	250.317	22.350	0.002695	146.202	0.5279
-2.750	-0.4080	2.20	24.5	291.604	231.414	20.644	0.002490	135.041	0.4876
-2.500	-0.3709	2.12	24.5	270.782	210.542	18.765	0.002263	122.751	0.4432
-2.250	-0.3338	2.02	25.5	245.839	190.648	18.636	0.002248	121.909	0.4402
-1.125	-0.1669	2.02	24.6	245.839	186.055	16.717	0.002016	109.353	0.3948
-1.000	-0.1484	2.12	24.5	270.782	210.542	18.765	0.002263	122.751	0.4432
-1.000	-0.1484	2.20	24.5	291.604	231.414	20.644	0.002490	135.041	0.4876
-0.938	-0.1391	2.27	24.5	310.456	250.317	22.350	0.002695	146.202	0.5279
-0.875	-0.1298	2.36	24.5	335.562	275.575	24.671	0.002975	161.387	0.5827
-0.813	-0.1205	2.45	24.6	361.643	301.809	27.092	0.003267	177.226	0.6399
-0.750	-0.1113	2.53	24.7	385.646	326.523	29.684	0.003580	194.179	0.7011
-0.688	-0.1020	2.76	25.2	458.951	402.378	38.322	0.004622	250.684	0.9051
-0.625	-0.0927	2.86	25.3	492.811	436.749	41.995	0.005065	274.713	0.9919
-0.500	-0.0742	2.97	25.4	531.448	475.898	46.204	0.005572	302.245	1.0913
-0.375	-0.0556	3.42	25.9	704.694	651.711	66.501	0.008020	435.021	1.5707
-0.313	-0.0464	3.64	26.0	798.272	745.701	76.718	0.009253	501.857	1.8120
0.250	0.0371	4.36	25.9	1145.305	1092.477	111.820	0.013486	731.474	2.5312
0.500	0.0742	3.64	26.0	798.272	745.701	76.718	0.009253	501.857	1.8120
0.625	0.0927	3.42	25.9	704.694	651.711	66.501	0.008020	435.021	1.5707
0.750	0.1113	3.17	25.8	605.434	552.142	55.998	0.006754	366.316	1.3226
1.750	0.2596	3.05	25.5	560.464	505.426	49.552	0.005976	324.145	1.1704
2.250	0.3338	2.97	25.4	531.448	475.898	46.204	0.005572	302.245	1.0913
3.750	0.5564	2.86	25.3	492.811	436.749	41.995	0.005065	274.713	0.9919
4.000	0.5935	2.76	25.2	458.951	402.378	38.322	0.004622	250.684	0.9051
4.500	0.6677	2.63	25.0	416.735	359.140	33.564	0.004048	219.564	0.7928
5.300	0.7864	2.53	24.7	385.646	326.523	29.684	0.003580	194.179	0.7011
5.750	0.8531	2.45	24.6	361.643	301.809	27.092	0.003267	177.226	0.6399
6.000	0.8902	2.36	24.5	335.562	275.575	24.671	0.002975	161.387	0.5827
6.250	0.9273	2.27	24.5	310.456	250.317	22.350	0.002695	146.202	0.5279
6.500	0.9644	2.20	24.5	291.604	231.414	20.644	0.002490	135.041	0.4876
6.800	1.0089	2.12	24.5	270.782	210.542	18.765	0.002263	122.751	0.4432
7.250	1.0757	2.02	24.6	245.839	186.055	16.717	0.002016	109.353	0.3948
7.500	1.1128	2.12	24.5	270.782	210.542	18.765	0.002263	122.751	0.4432
7.750	1.1499	2.20	24.5	291.604	231.414	20.644	0.002490	135.041	0.4876
7.750	1.1499	2.27	24.5	310.456	250.317	22.350	0.002695	146.202	0.5279
7.750	1.1499	2.36	24.5	335.562	275.575	24.671	0.002975	161.387	0.5827
7.800	1.1573	2.45	24.6	361.643	301.809	27.092	0.003267	177.226	0.6399
8.000	1.1869	2.53	24.7	385.646	326.523	29.684	0.003580	194.179	0.7011
8.100	1.2018	2.63	25.0	416.735	359.140	33.564	0.004048	219.564	0.7928
8.250	1.2240	2.76	25.2	458.951	402.378	38.322	0.004622	250.684	0.9051
8.500	1.2611	2.86	25.3	492.811	436.749	41.995	0.005065	274.713	0.9919
8.500	1.2611	2.97	25.4	531.448	475.898	46.204	0.005572	302.245	1.0913
8.750	1.2982	3.05	25.5	560.464	505.426	49.552	0.005976	324.145	1.1704
9.500	1.4095	2.97	25.4	531.448	475.898	46.204	0.005572	302.245	1.0913
10.500	1.5579	3.05	25.5	560.464	505.426	49.552	0.005976	324.145	1.1704

Clean Tunnel Configuration

$T_u = 0.5\%$



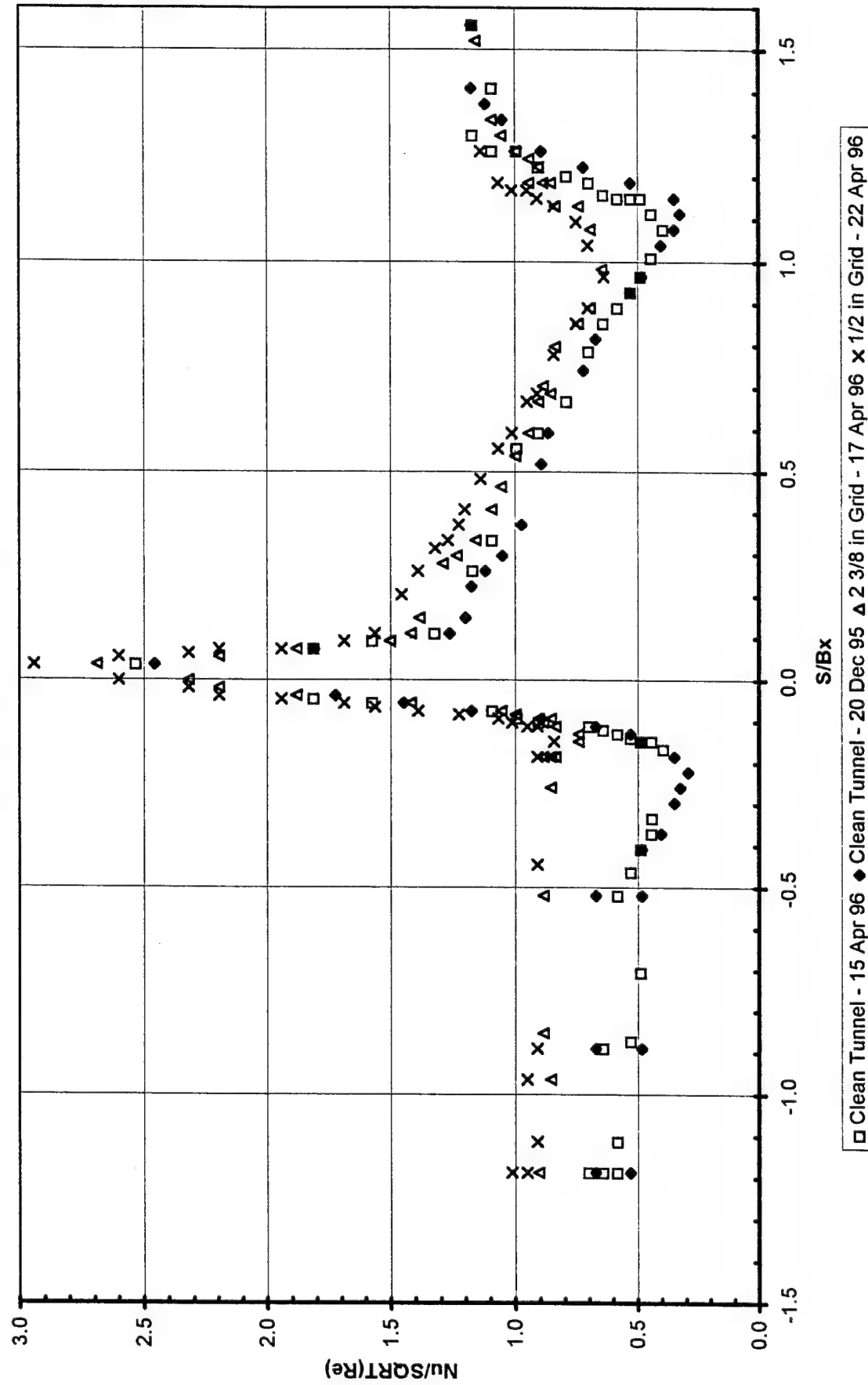
A2

P inf =	11.400	psi		Rho =	0.9178	kg/m^3			
T inf =	25.400	C		Mu =	1.8384E-05	N s/m^2			
T lc =	35.700	C		k air =	0.0262	W/mK			
Delta P =	0.301	torr		V inf =	9.344	m/s			
L =	18.531	in		Bx =	6.740	in			
W =	8.039	in		Re =	79855.6				
R" =	2.512	Ohms/SQ		Cond. =	0	W/m^2			
Emiss. =	0.850			S-B Con. =	5.670E-08	W/m^2K^4			
1/2 in Grid at 15 in -			1/2 in Grid - 22 Apr 96						
s (in)	s/Bx	Current (Amps)	T inf (C)	q" (W/m^2)	qc" (W/m^2)	h (W/m^2K)	St	Nu	Nu/SQRT(Re)
-8.000	-1.1869	2.81	25.5	475.730	420.539	41.108	0.004760	268.799	0.9512
-8.000	-1.1869	2.89	25.5	503.204	447.910	43.699	0.005060	285.735	1.0111
-7.500	-1.1128	2.76	25.4	458.951	403.606	39.338	0.004555	257.222	0.9102
-6.500	-0.9644	2.81	25.5	475.730	420.539	41.108	0.004760	268.799	0.9512
-6.000	-0.8902	2.76	25.4	458.951	403.606	39.338	0.004555	257.222	0.9102
-3.000	-0.4451	2.76	25.4	458.951	403.606	39.338	0.004555	257.222	0.9102
-1.250	-0.1855	2.76	25.4	458.951	403.606	39.338	0.004555	257.222	0.9102
-1.000	-0.1484	2.67	25.5	429.507	374.213	36.509	0.004228	238.722	0.8448
-0.750	-0.1113	2.76	25.4	458.951	403.606	39.338	0.004555	257.222	0.9102
-0.750	-0.1113	2.81	25.5	475.730	420.539	41.108	0.004760	268.799	0.9512
-0.688	-0.1020	2.89	25.5	503.204	447.910	43.699	0.005060	285.735	1.0111
-0.625	-0.0927	2.96	25.5	527.876	472.582	46.106	0.005339	301.474	1.0668
-0.563	-0.0835	3.16	25.4	601.620	546.070	53.016	0.006139	346.664	1.2267
-0.500	-0.0742	3.35	25.4	676.142	620.438	60.062	0.006955	392.731	1.3898
-0.438	-0.0649	3.52	25.5	746.506	691.264	67.506	0.007817	441.409	1.5620
-0.375	-0.0556	3.66	25.4	807.068	751.467	72.887	0.008440	476.594	1.6865
-0.313	-0.0464	3.94	25.2	935.278	878.858	83.941	0.009720	548.870	1.9423
-0.250	-0.0371	4.15	25.4	1037.634	981.828	94.863	0.010985	620.287	2.1950
-0.125	-0.0185	4.26	25.4	1093.370	1037.616	100.350	0.011621	656.165	2.3220
0.000	0.0000	4.50	25.3	1220.037	1164.180	112.373	0.013013	734.781	2.6002
0.250	0.0371	4.78	25.3	1376.588	1320.577	127.101	0.014718	831.085	2.9410
0.375	0.0556	4.50	25.3	1220.037	1164.180	112.373	0.013013	734.781	2.6002
0.438	0.0649	4.26	25.4	1093.370	1037.616	100.350	0.011621	656.165	2.3220
0.500	0.0742	3.94	25.2	935.278	878.858	83.941	0.009720	548.870	1.9423
0.500	0.0742	4.15	25.4	1037.634	981.828	94.863	0.010985	620.287	2.1950
0.625	0.0927	3.66	25.4	807.068	751.467	72.887	0.008440	476.594	1.6865
0.750	0.1113	3.52	25.5	746.506	691.264	67.506	0.007817	441.409	1.5620
1.375	0.2040	3.43	25.3	708.821	652.810	62.831	0.007276	410.836	1.4538
1.750	0.2596	3.35	25.4	676.142	620.438	60.062	0.006955	392.731	1.3898
2.125	0.3153	3.26	25.5	640.300	585.006	57.074	0.006609	373.193	1.3206
2.250	0.3338	3.21	25.4	618.877	563.532	54.925	0.006360	359.144	1.2709
2.500	0.3709	3.16	25.4	601.620	546.070	53.016	0.006139	346.664	1.2267
2.750	0.4080	3.12	25.5	586.486	531.345	51.991	0.006021	339.957	1.2030
3.250	0.4822	3.06	25.4	564.145	508.339	49.115	0.005688	321.152	1.1365
3.750	0.5564	2.96	25.5	527.876	472.582	46.106	0.005339	301.474	1.0668
4.000	0.5935	2.89	25.5	503.204	447.910	43.699	0.005060	285.735	1.0111
4.500	0.6677	2.81	25.5	475.730	420.539	41.108	0.004760	268.799	0.9512
4.625	0.6862	2.76	25.4	458.951	403.606	39.338	0.004555	257.222	0.9102
5.250	0.7789	2.67	25.5	429.507	374.213	36.509	0.004228	238.722	0.8448
5.750	0.8531	2.56	25.3	394.846	338.784	32.575	0.003772	213.004	
6.000	0.8902	2.47	25.4	367.572	312.226	30.431	0.003524	198.985	0.7538
6.500	0.9644	2.38	25.4	341.273	285.518	27.613	0.003198	180.555	0.6389
7.000	1.0386	2.47	25.4	367.572	312.226	30.431	0.003524	198.985	0.7042
7.375	1.0942	2.56	25.3	394.846	338.784	32.575	0.003772	213.004	0.7538
7.625	1.1313	2.67	25.5	429.507	374.213	36.509	0.004228	238.722	0.8448
7.750	1.1499	2.76	25.4	458.951	403.606	39.338	0.004555	257.222	0.9102
7.875	1.1684	2.81	25.5	475.730	420.539	41.108	0.004760	268.799	0.9512
7.875	1.1684	2.89	25.5	503.204	447.910	43.699	0.005060	285.735	1.0111
8.000	1.1869	2.96	25.5	527.876	472.582	46.106	0.005339	301.474	1.0668
8.500	1.2611	3.06	25.4	564.145	508.339	49.115	0.005688	321.152	1.1365

P inf =	11.280	psi		Rho =	0.9093	kg/m^3				
T inf =	25.000	C		Mu =	1.8365E-05	N s/m^2				
T lc =	35.700	C		k air =	0.0262	W/mK				
Delta P =	0.323	torr		V inf =	9.732	m/s				
L =	18.531	in		Bx =	6.740	in				
W =	8.039	in		Re =	82494.8					
R" =	2.512	Ohms/SQ		Cond. =	0	W/m^2				
Emmis. =	0.850			S-B Con. =	5.670E-08	W/m^2K^4				
Clean Tunnel Stagnation Points -			01 May 96, 15 Apr 96, & 20 Dec 96							
s (in)	s/Bx	Current (Amps)	T inf (C)	q" (W/m^2)	qc" (W/m^2)	h (W/m^2K)	St	Nu	Nu/SQRT(Re)	
0.250	0.0371	4.12	27.1	1022.687	975.762	113.066	0.012687	740.154	2.5770	
0.250	0.0371	3.54	29.4	755.013	720.473	114.725	0.012874	751.012	2.6148	
0.250	0.0371	4.95	22.8	1476.245	1407.302	108.672	0.012194	711.388	2.4768	
0.250	0.0371	4.36	25.9	1145.305	1092.477	111.820	0.013486	731.474	2.6411	
0.250	0.0371	4.55	24.4	1247.300	1186.654	105.014	0.012385	688.608	2.4560	

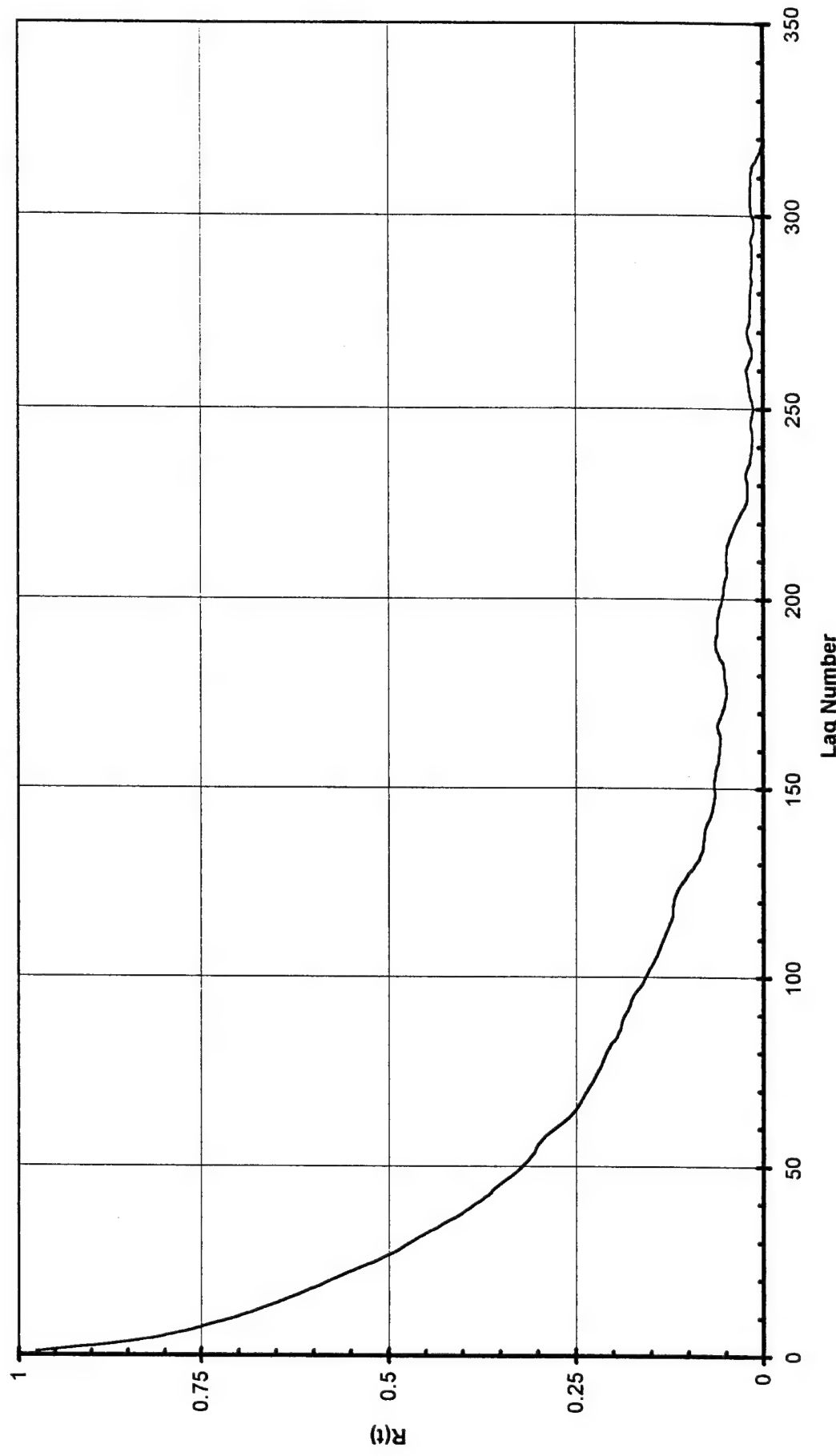
**Appendix B:
Heat Transfer Data Sheets**

Heat Transfer Comparison



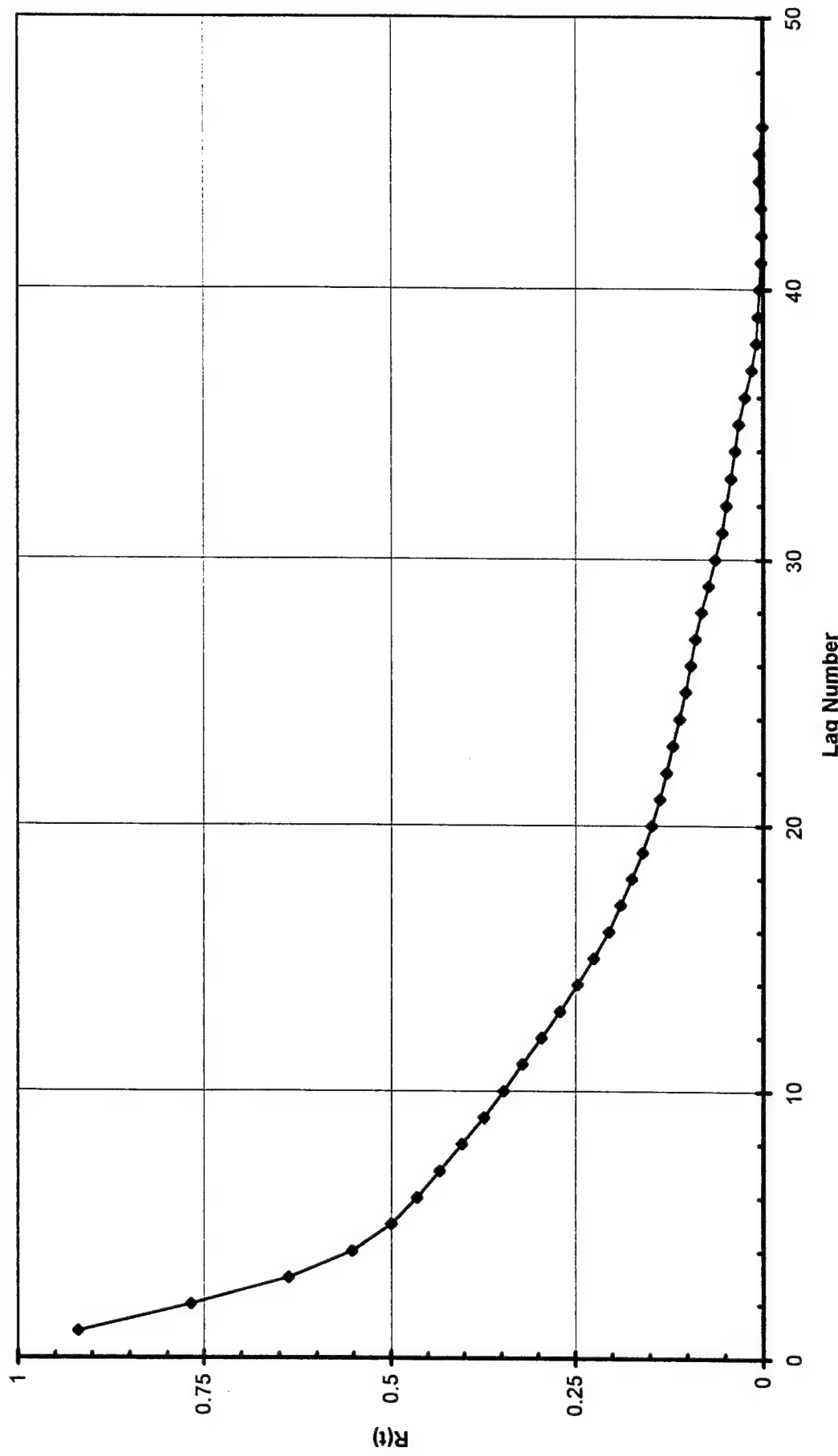
**Appendix C:
Length Scale Data Sheets**

Autocorrelation Results
2 3/8 in Grid at 72 3/4 in



C1

Autocorrelation Results
1/2 in Grid at 15 in.



C2

Integral Length Scale				
Lag	Corr.	Average	U =	8.658 m/s
1	0.976	0.9505	Freq =	6000 Hz
2	0.925	0.8995	Integral =	0.070532 m
3	0.874	0.854		2.776866 in
4	0.834	0.8195		
5	0.805	0.793		
6	0.781	0.7705	Micro-length Scale	
7	0.76	0.7505	Lag 1 =	0.995
8	0.741	0.732	Freq =	15000 Hz
9	0.723	0.7145	U =	8.882 m/s
10	0.706	0.698	Micro =	0.008374 m
11	0.69	0.683		0.329686 in
12	0.676	0.669		
13	0.662	0.655		
14	0.648	0.6415		
15	0.635	0.6285		
16	0.622	0.616		
17	0.61	0.604		
18	0.598	0.5925		
19	0.587	0.5815		
20	0.576	0.5705		
21	0.565	0.559		
22	0.553	0.547		
23	0.541	0.5345		
24	0.528	0.522		
25	0.516	0.5105		
26	0.505	0.5		
27	0.495	0.4905		
28	0.486	0.482		
29	0.478	0.474		
30	0.47	0.4655		
31	0.461	0.4565		
32	0.452	0.447		
33	0.442	0.4375		
34	0.433	0.4285		
35	0.424	0.4195		
36	0.415	0.4105		
37	0.406	0.402		
38	0.398	0.3945		
39	0.391	0.3875		
40	0.384	0.38		
41	0.376	0.3725		
42	0.369	0.366		
43	0.363	0.3605		
44	0.358	0.355		
45	0.352	0.3485		
46	0.345	0.3415		
47	0.338	0.335		
48	0.332	0.329		
49	0.326	0.3235		
50	0.321	0.3185		
51	0.316	0.314		
52	0.312	0.31		
53	0.308	0.306		
54	0.304	0.303		
55	0.302	0.3005		
56	0.299	0.297		
57	0.295	0.2925		
58	0.29	0.287		
59	0.284	0.2805		
60	0.277	0.274		
61	0.271	0.2675		

62	0.264	0.2615
63	0.259	0.2565
64	0.254	0.252
65	0.25	0.2485
66	0.247	0.2455
67	0.244	0.2425
68	0.241	0.2395
69	0.238	0.2365
70	0.235	0.2335
71	0.232	0.2305
72	0.229	0.2275
73	0.226	0.2245
74	0.223	0.222
75	0.221	0.2195
76	0.218	0.217
77	0.216	0.215
78	0.214	0.213
79	0.212	0.211
80	0.21	0.2085
81	0.207	0.2055
82	0.204	0.202
83	0.2	0.198
84	0.196	0.195
85	0.194	0.193
86	0.192	0.191
87	0.19	0.1895
88	0.189	0.188
89	0.187	0.186
90	0.185	0.1835
91	0.182	0.181
92	0.18	0.179
93	0.178	0.177
94	0.176	0.175
95	0.174	0.1725
96	0.171	0.169
97	0.167	0.165
98	0.163	0.1615
99	0.16	0.159
100	0.158	0.1565
101	0.155	0.154
102	0.153	0.1515
103	0.15	0.1485
104	0.147	0.146
105	0.145	0.1435
106	0.142	0.141
107	0.14	0.139
108	0.138	0.137
109	0.136	0.135
110	0.134	0.133
111	0.132	0.131
112	0.13	0.129
113	0.128	0.127
114	0.126	0.125
115	0.124	0.123
116	0.122	0.1215
117	0.121	0.121
118	0.121	0.121
119	0.121	0.1205
120	0.12	0.1195
121	0.119	0.118
122	0.117	0.116
123	0.115	0.1135
124	0.112	0.1105
125	0.109	0.107
126	0.105	0.1035

127	0.102	0.1			
128	0.098	0.096			
129	0.094	0.0925			
130	0.091	0.089			
131	0.087	0.086			
132	0.085	0.084			
133	0.083	0.082			
134	0.081	0.0805			
135	0.08	0.08			
136	0.08	0.0795			
137	0.079	0.079			
138	0.079	0.0785			
139	0.078	0.0775			
140	0.077	0.076			
141	0.075	0.0735			
142	0.072	0.071			
143	0.07	0.0695			
144	0.069	0.0685			
145	0.068	0.0675			
146	0.067	0.0665			
147	0.066	0.0655			
148	0.065	0.065			
149	0.065	0.0655			
150	0.066	0.066			
151	0.066	0.066			
152	0.066	0.0655			
153	0.065	0.0645			
154	0.064	0.0635			
155	0.063	0.0625			
156	0.062	0.061			
157	0.06	0.06			
158	0.06	0.0595			
159	0.059	0.0585			
160	0.058	0.058			
161	0.058	0.0575			
162	0.057	0.057			
163	0.057	0.0575			
164	0.058	0.059			
165	0.06	0.0605			
166	0.061	0.061			
167	0.061	0.06			
168	0.059	0.058			
169	0.057	0.056			
170	0.055	0.0545			
171	0.054	0.053			
172	0.052	0.0515			
173	0.051	0.0505			
174	0.05	0.0495			
175	0.049	0.049			
176	0.049	0.0495			
177	0.05	0.0505			
178	0.051	0.0515			
179	0.052	0.052			
180	0.052	0.052			
181	0.052	0.0525			
182	0.053	0.0535			
183	0.054	0.0555			
184	0.057	0.058			
185	0.059	0.06			
186	0.061	0.062			
187	0.063	0.0635			
188	0.064	0.064			
189	0.064	0.0635			
190	0.063	0.062			
191	0.061	0.061			

192	0.061	0.061				
193	0.061	0.061				
194	0.061	0.061				
195	0.061	0.0605				
196	0.06	0.0595				
197	0.059	0.0585				
198	0.058	0.057				
199	0.056	0.0555				
200	0.055	0.0545				
201	0.054	0.0535				
202	0.053	0.053				
203	0.053	0.0525				
204	0.052	0.0515				
205	0.051	0.05				
206	0.049	0.0485				
207	0.048	0.048				
208	0.048	0.0485				
209	0.049	0.049				
210	0.049	0.049				
211	0.049	0.049				
212	0.049	0.0485				
213	0.048	0.048				
214	0.048	0.047				
215	0.046	0.0455				
216	0.045	0.044				
217	0.043	0.042				
218	0.041	0.04				
219	0.039	0.038				
220	0.037	0.0355				
221	0.034	0.0325				
222	0.031	0.03				
223	0.029	0.0275				
224	0.026	0.025				
225	0.024	0.023				
226	0.022	0.0215				
227	0.021	0.021				
228	0.021	0.021				
229	0.021	0.021				
230	0.021	0.0215				
231	0.022	0.0225				
232	0.023	0.023				
233	0.023	0.0225				
234	0.022	0.021				
235	0.02	0.019				
236	0.018	0.0175				
237	0.017	0.0165				
238	0.016	0.0155				
239	0.015	0.015				
240	0.015	0.0145				
241	0.014	0.014				
242	0.014	0.014				
243	0.014	0.0145				
244	0.015	0.0155				
245	0.016	0.016				
246	0.016	0.016				
247	0.016	0.0155				
248	0.015	0.0145				
249	0.014	0.0135				
250	0.013	0.0135				
251	0.014	0.0145				
252	0.015	0.016				
253	0.017	0.0175				
254	0.018	0.0185				
255	0.019	0.0195				
256	0.02	0.02				

257	0.02	0.0205		
258	0.021	0.0215		
259	0.022	0.0225		
260	0.023	0.022		
261	0.021	0.02		
262	0.019	0.018		
263	0.017	0.016		
264	0.015	0.015		
265	0.015	0.0155		
266	0.016	0.017		
267	0.018	0.019		
268	0.02	0.0205		
269	0.021	0.0215		
270	0.022	0.0215		
271	0.021	0.02		
272	0.019	0.0185		
273	0.018	0.018		
274	0.018	0.018		
275	0.018	0.018		
276	0.018	0.0175		
277	0.017	0.017		
278	0.017	0.017		
279	0.017	0.017		
280	0.017	0.0165		
281	0.016	0.016		
282	0.016	0.0155		
283	0.015	0.0155		
284	0.016	0.016		
285	0.016	0.016		
286	0.016	0.0155		
287	0.015	0.015		
288	0.015	0.015		
289	0.015	0.015		
290	0.015	0.015		
291	0.015	0.015		
292	0.015	0.0155		
293	0.016	0.016		
294	0.016	0.0155		
295	0.015	0.014		
296	0.013	0.0125		
297	0.012	0.012		
298	0.012	0.0125		
299	0.013	0.014		
300	0.015	0.0155		
301	0.016	0.016		
302	0.016	0.0165		
303	0.017	0.017		
304	0.017	0.017		
305	0.017	0.017		
306	0.017	0.017		
307	0.017	0.0165		
308	0.016	0.016		
309	0.016	0.016		
310	0.016	0.016		
311	0.016	0.0155		
312	0.015	0.0145		
313	0.014	0.0125		
314	0.011	0.01		
315	0.009	0.0075		
316	0.006	0.005		
317	0.004	0.0035		
318	0.003	0.002		
319	0.001	0.0005		

Integral Length Scale					
Lag	Corr.	Average	U =	9.347	m/s
1	0.919	0.8435	Freq =	6000	Hz
2	0.768	0.703	Integral =	0.013199	m
3	0.638	0.595		0.519636	in
4	0.552	0.526			
5	0.5	0.4825			
6	0.465	0.4495	Micro-length Scale		
7	0.434	0.419	Lag 1 =	0.985	
8	0.404	0.389	Freq =	15000	Hz
9	0.374	0.3605	U =	8.998	m/s
10	0.347	0.3345	Micro =	0.004898	m
11	0.322	0.309		0.19283	in
12	0.296	0.2835			
13	0.271	0.259			
14	0.247	0.236			
15	0.225	0.215			
16	0.205	0.197			
17	0.189	0.1815			
18	0.174	0.167			
19	0.16	0.154			
20	0.148	0.1425			
21	0.137	0.1325			
22	0.128	0.124			
23	0.12	0.1155			
24	0.111	0.107			
25	0.103	0.0995			
26	0.096	0.093			
27	0.09	0.086			
28	0.082	0.077			
29	0.072	0.0675			
30	0.063	0.0585			
31	0.054	0.051			
32	0.048	0.045			
33	0.042	0.0395			
34	0.037	0.0345			
35	0.032	0.028			
36	0.024	0.0195			
37	0.015	0.012			
38	0.009	0.008			
39	0.007	0.006			
40	0.005	0.004			
41	0.003	0.0025			
42	0.002	0.0025			
43	0.003	0.004			
44	0.005	0.005			
45	0.005	0.003			
46	0.001	0.0005			

Appendix D: Uncertainty Analysis

			% Uncertainty	q" Uncertainty	% q"	qc"	% qc"	h Uncertainty	% h Uncertainty
Current	5.00 +/- 0.0050 Amps		0.10	3.01	0.20	3.01	0.21	0.28	0.21
Resistance	2.51 +/- 0.1256 Ohms/sq		5.00	75.31	5.00	75.31	5.20	7.04	5.20
Film Width	0.20 +/- 0.0002 m		0.10	-2.93	-0.19	-2.93	-0.20	-0.27	-0.20
T inf	25.00 +/- 0.1500 deg C		0.60	Not Used	Not Used	0.77	0.05	1.97	1.45
T LC	35.70 +/- 0.1500 deg C		0.42	Not Used	Not Used	-0.85	-0.06	-1.98	-1.46
Emmissivity	0.85 +/- 0.1500		17.65	Not Used	Not Used	-10.16	-0.70	-0.95	-0.70
Conduction	0.00 +/- 0.0000 W/m^2		0.00	Not Used	Not Used	0.00	0.00	0.00	0.00
S-B Const	5.67E-08 W/(m^2*K^4)								
q" =	1506.219 +/- 75.428 W/m^2			5.01 % Uncertainty					
qc" =	1448.624 +/- 76.118 W/m^2			5.25 % Uncertainty					
h =	135.385 +/- 7.641 W/(m^2*K)			5.64 % Uncertainty					
			% Uncertainty	q" Uncertainty	% q"	qc"	% qc"	h Uncertainty	% h Uncertainty
Current	2.00 +/- 0.0050 Amps		0.25	1.20	0.50	1.20	0.66	0.11	0.66
Resistance	2.51 +/- 0.1256 Ohms/sq		5.00	12.05	5.00	12.05	6.57	1.13	6.57
Film Width	0.20 +/- 0.0002 m		0.10	-0.47	-0.19	-0.47	-0.26	-0.04	-0.26
T inf	25.00 +/- 0.1500 deg C		0.60	Not Used	Not Used	0.77	0.42	0.31	1.82
T LC	35.70 +/- 0.1500 deg C		0.42	Not Used	Not Used	-0.85	-0.46	-0.32	-1.87
Emmissivity	0.85 +/- 0.1500		17.65	Not Used	Not Used	-10.16	-5.54	-0.95	-5.54
Conduction	0.00 +/- 0.0000 W/m^2		0.00	Not Used	Not Used	0.00	0.00	0.00	0.00
S-B Const	5.67E-08 W/(m^2*K^4)								
q" =	240.995 +/- 12.119 W/m^2			5.03 % Uncertainty					
qc" =	183.400 +/- 15.858 W/m^2			8.65 % Uncertainty					
h =	17.140 +/- 1.544 W/(m^2*K)			9.01 % Uncertainty					